

# FLOWS OF VISCOPLASTIC MATERIALS: MODELS AND COMPUTATIONS

**Evan Mitsoulis**

School of Mining Engineering and Metallurgy  
National Technical University of Athens  
Zografou, 157 80 Athens, Greece

## ABSTRACT

Viscoplasticity is characterized by a yield stress, below which the materials will not deform, and above which they will deform and flow according to different constitutive relations. Viscoplastic models include the Bingham plastic, the Herschel-Bulkley model, and the Casson model. All of these ideal models are discontinuous. Analytical solutions exist for such models in simple flows. For general flow fields, it is necessary to develop numerical techniques to track down yielded/unyielded regions. This can be avoided by introducing into the models a continuation parameter, which facilitates the solution process and produces virtually the same results as the ideal models by the right choice of its value. This work reviews several benchmark problems of viscoplastic flows, such as entry and exit flows from dies, flows around a sphere and a cylinder, and squeeze flows. Examples are also given for typical processing flows of viscoplastic materials, where the extent and shape of the yielded/unyielded regions are clearly shown.

**KEYWORDS:** Viscoplastic fluids, Bingham plastics, Herschel-Bulkley fluids, viscoplastic models, simulations, yield stress, yielded/unyielded regions

---

## 1. INTRODUCTION

During the past several decades the emphasis in rheology and continuum mechanics had been on one-phase materials, with particular attention to polymer solutions and polymer melts [1]. Slurries, pastes, and suspensions, frequently encountered in industrial problems, had received less attention than they deserved. Many of these materials have a *yield stress*, a critical value of stress below which they do not flow; they are sometimes called *viscoplastic materials* or *Bingham plastics*, after Bingham [2], who was the first to describe several types of paint in this way in 1919. They constitute an important class of non-Newtonian materials.

The situation appears to have gradually changed after the appearance in 1983 of a seminal review paper by Bird et al. [1]. In that work, the authors provide a list of

several materials exhibiting yield, including examples from the food industry, such as margarine, mayonnaise and ketchup, examples of suspensions in Newtonian fluids, etc. They have also made a comprehensive effort to collect most of the works related to viscoplastic materials up to 1980, amounting to 214 references. They have included theoretical developments based on viscoplastic models. The models presented for such so-called viscoplastic materials included the Bingham [2], Herschel-Bulkley [3] and Casson [4]. Analytical solutions were provided for the Bingham plastic model in simple flow fields.

Since then, a renewed interest has surfaced among several researchers to study these materials in non-trivial flows, either experimentally or theoretically, including both modelling and simulation efforts. Around the early 1980s, and due to the availability of 2-D computer codes for solving flow problems [5-10], the first attempts were made to address modifications in the modelling and the subsequent numerical simulation of benchmark problems of Bingham plastics. Thus, several modified models appeared to render the simulations affordable with varying degrees of success [11-13]. Meanwhile, and in parallel, experimentalists were making efforts to measure the rheological properties of viscoplastic materials, and in particular their dominant property of yield stress. Typical examples of such efforts made in 1980's can be found in the works by Covey and Stanmore [14], Keentok et al. [15], Boger and his co-workers [16-18], Magnin and Piau [19-20]. A review of experimental methods for yield stress fluids also appeared by Nguyen and Boger [21], encompassing most findings up to 1992. The difficulties of measuring the yield stress and of finding in experiments the unyielded regions were highlighted and remained challenges to be resolved. Meanwhile, there was a vivid discussion about the existence of the yield stress, with arguments both for and against. Barnes and Walters [22] concluded that no yield stress exists, that new instruments were exploding the yield-stress myth and asserted that no one ever measured a yield stress. They stated that if a material flows at high stresses it would also flow, however slowly at low stresses. However, this was disputed by Harnett and Hu [23], Schurz [24], and Astarita [25]. These authors argued for an engineering or empirical reality and its engineering implications.

Given these engineering realities, it was thought that viscoplastic materials can be well approximated uniformly at all levels of stress as liquids that exhibit infinitely high viscosity in the limit of low shear rates followed by a continuous transition to a viscous liquid. This approximation could be made more and more accurate at even vanishingly small shear rates by means of a material parameter that controls the exponential growth of stress. Thus, a new impetus was given in 1987 with the publication by Papanastasiou [26] of such a modification of the Bingham model with an exponential stress-growth term. The new model basically rendered the original discontinuous Bingham viscoplastic model as a purely viscous one, which was easy to implement and solve and was valid for all rates of deformation. The early efforts by Papanastasiou and his co-workers [26,27] were taken up by the author and his co-workers, who in a series of papers [28-44] solved many benchmark problems and presented useful solutions always providing the yielded/unyielded regions in flow fields of interest. Since the early 1990s, other workers in the field also used the Papanastasiou model for many different problems [45-52].

Meanwhile the experimental techniques have seen many improvements as evidenced by relevant works in the field [53-64]. The end of 1990s saw another general review on the subject of the yield stress in rheology by Barnes [65] citing 160 references, with the emphasis on experimental techniques and their pros and cons. Another subject related with viscoplasticity is the squeeze flow problem in a plastometer, for which there are many works as evidenced by a recent review in 2005 by Engmann et al. [66], which cites 200 references. Also in 2005, Frigaard and Nouar [67] published a review dealing with issues of modelling and simulations of viscoplastic materials. Most of the efforts in the theoretical analyses have been directed towards determining the extent and shape of yielded/unyielded regions, which are the pre-eminent feature of viscoplastic materials due to their yield stress. Because different criteria have been used by different researchers, a confusion existed regarding the determination of these regions, and this was reflected in the literature by different models and their implementation [67]. The work of Frigaard and Nouar [67] reviewed these models and showed that the continuous regularized Papanastasiou model provided the best approximation to the ideal discontinuous model, but it also failed in other aspects, for example in cases of stability analysis of viscoplastic flows. Indeed, the Papanastasiou model and its variants are predominantly used today and have been implemented in all major commercial fluid-flow packages for the simulation of viscoplastic flows. There are now more than 140 citations to the original work [26] up to the end of 2006, as evidenced by a search in the Web of Science, Institute for Scientific Information, ISI, [www.ekt.gr](http://www.ekt.gr) [68].

The subject of viscoplasticity is still considered a “hot” subject, worthy of further research and development. This was borne out in a workshop on “Visco-plastic fluids: from theory to applications”, which was held in Banff, Canada, in October 2005, and in which about 40 researchers participated from around the world. Selected papers appeared in a special issue of the *Journal of Non-Newtonian Fluid Mechanics* [69]. The 2nd workshop took place in Monte Verita, Switzerland, in October 2007, attracting some 70 participants. The 3rd workshop is scheduled for November 2009 in Limassol, Cyprus.

In the time elapsed between the review work of Bird et al. [1] in 1983 and that of Frigaard and Nouar [67] in 2005, i.e., in one generation, more than 1000 scientific papers on the subject of viscoplastic fluids have appeared (ISI, Web of Science, keywords in title: viscoplastic fluid, Bingham fluid, Bingham plastic, Herschel-Bulkley fluid) [68]. This is an indication of the great interest in the subject, which is bound to grow as more synergy is expected from various –and apparently diverse– fields, extending from lava flows to mayonnaise spreading.

Due to this ever-growing body of knowledge, it is impossible to account for all aspects of viscoplastic materials in the confines of a review article of limited size. Thus, the present work will focus on the modelling and simulation aspects for viscoplastic fluids, and in particular on some (apparently) simple benchmark problems solved by different models and methods. The emphasis will be on finding the extent and shape of yielded/unyielded regions, as these are predicted by the simulations, while some comments and thoughts will be dedicated to future developments in this important subject of rheology.

## 2. MATHEMATICAL MODELLING

The flow is governed by the usual conservation equations of mass, momentum and energy for incompressible fluids and laminar flow (see, e.g., [1,70,71]). To model the stress-deformation behaviour of viscoplastic materials, different constitutive equations have been proposed [1]. In simple shear flow these take the form (Figure 1):

*Bingham plastic model:*

$$\tau = \tau_y + \mu\dot{\gamma} \quad \text{for } |\tau| > \tau_y \quad (1)$$

*Herschel-Bulkley model:*

$$\tau = \tau_y + K\dot{\gamma}^n \quad \text{for } |\tau| > \tau_y \quad (2)$$

*Casson model:*

$$\sqrt{\tau} = \sqrt{\tau_y} + \sqrt{\mu\dot{\gamma}} \quad \text{for } |\tau| > \tau_y \quad (3)$$

For all models, we have:

$$\dot{\gamma} = 0 \quad \text{for } |\tau| \leq \tau_y \quad (4)$$

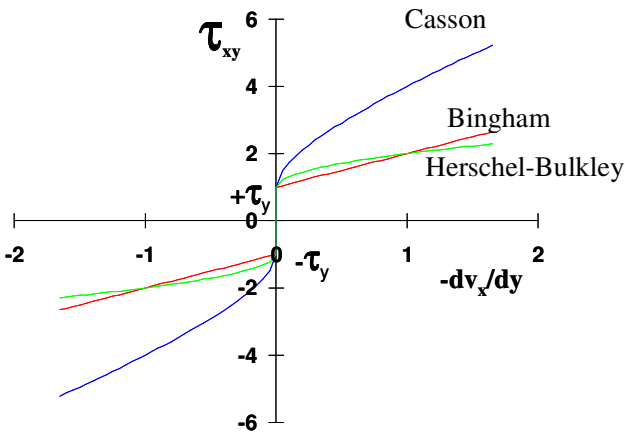


**Figure 1:** Shear stress ( $\tau_{xy}$ ) vs. shear rate ( $\dot{\gamma}_{xy} = dv_x/dy$ ) for different types of viscoplastic models.

In the above,  $\tau$  is the shear stress,  $\dot{\gamma}=dv_x/dy$  is the shear rate,  $\tau_y$  is the yield stress,  $\mu$  is a constant plastic viscosity,  $K$  is the consistency index, and  $n$  is the power-law index. Note that when the shear stress  $\tau$  falls below  $\tau_y$ , a solid structure is formed (unyielded).

In order to express these equations as fully invariant constitutive relations applicable in three dimensions, tensors are introduced [72]. Then the above models are written as:

*Bingham plastic model:*

$$\bar{\tau} = \left( \mu + \frac{\tau_y}{|\dot{\gamma}|} \right) \bar{\dot{\gamma}} \quad \text{for } |\tau| > \tau_y \quad (5)$$

*Herschel-Bulkley model:*

$$\bar{\tau} = \left( K |\dot{\gamma}|^{n-1} + \frac{\tau_y}{|\dot{\gamma}|} \right) \bar{\dot{\gamma}} \quad \text{for } |\tau| > \tau_y \quad (6)$$

*Casson model:*

$$\bar{\tau} = \left( \sqrt{\mu} + \sqrt{\frac{\tau_y}{|\dot{\gamma}|}} \right)^2 \bar{\dot{\gamma}} \quad \text{for } |\tau| > \tau_y \quad (7)$$

For all models, we have:

$$\bar{\dot{\gamma}} = 0 \quad \text{for } |\tau| \leq \tau_y \quad (8)$$

In the above,  $|\dot{\gamma}|$  is the magnitude of the symmetric rate-of-strain tensor  $\bar{\dot{\gamma}} = \nabla \bar{v} + \nabla \bar{v}^T$ , which is given by

$$|\dot{\gamma}| = \sqrt{\frac{1}{2} II_{\dot{\gamma}}} = \left[ \frac{1}{2} \{ \bar{\dot{\gamma}} : \bar{\dot{\gamma}} \} \right]^{1/2} \quad (9)$$

where  $II_{\dot{\gamma}}$  is the second invariant of  $\bar{\dot{\gamma}}$ ,  $\nabla \bar{v}$  is the velocity gradient tensor and  $\nabla \bar{v}^T$  is its transpose. Similarly,  $|\tau|$  is the magnitude of the extra stress tensor  $\bar{\tau}$  given by:

$$|\tau| = \sqrt{\frac{1}{2} II_{\tau}} = \left[ \frac{1}{2} \{ \bar{\tau} : \bar{\tau} \} \right]^{1/2} \quad (10)$$

where  $II_{\tau}$  is the second invariant of  $\bar{\tau}$ .

It follows from the above that the criterion to track down yielded/unyielded regions is for the material to flow (yield) only when the magnitude of the extra stress tensor  $|\tau|$  exceeds the yield stress  $\tau_y$ , i.e.,

$$\text{yielded:} \quad |\tau| = \sqrt{\frac{1}{2} II_{\tau}} = \left[ \frac{1}{2} \{ \bar{\tau} : \bar{\tau} \} \right]^{1/2} > \tau_y \quad (11a)$$

$$\text{unyielded:} \quad |\tau| = \sqrt{\frac{1}{2} II_{\tau}} = \left[ \frac{1}{2} \{ \bar{\tau} : \bar{\tau} \} \right]^{1/2} \leq \tau_y \quad (11b)$$

The three-dimensional formulation is necessary for the solution of problems in more than one dimensions. Below are given the key works that allowed such solutions, together with the various modifications made to the original ideal Bingham model in order to avoid the discontinuity.

(A) *Bercovier and Engelman* [5]: A two-dimensional analysis was first attempted by Bercovier and Engelman [5] in 1980, who, in order to avoid the model discontinuity, wrote it as:

$$\bar{\tau} = \left( \mu + \frac{\tau_y}{|\dot{\gamma}| + e} \right) \dot{\gamma} \quad \text{for } |\tau| > \tau_y \quad (12)$$

where  $e$  is a regularization parameter, which is a very small number, e.g.,  $e = 10^{-3} \text{ s}^{-1}$ . Obviously, eq. (8) is valid for  $|\dot{\gamma}| = e$ . Thus, Bercovier and Engelman [5] solved a benchmark 2-D problem of that time (flow in a lid-driven square cavity), but did not give yielded/unyielded regions according to the criterion of the yield stress  $|\tau| = \tau_y$ . Instead they presented contours of  $|\dot{\gamma}| = e$ .

(B) *Tanner and Milthorpe* [7]: A second effort was made by Tanner and Milthorpe [7] in 1983, who regularized the ideal Bingham model with the so-called *bi-viscosity model*, having two finite viscosity slopes (i.e., two Newtonian models),  $\mu_o$  for  $|\dot{\gamma}| < \dot{\gamma}_c$ , and  $\mu$  for  $|\dot{\gamma}| > \dot{\gamma}_c$ . After many trials of checking the results against the analytical 1-D solution for Poiseuille flow, the optimal values were found to be  $\mu_o = 1000\mu$  and  $\dot{\gamma}_c = 10^{-3} \text{ s}^{-1}$ . The behaviour of this model in simple shear flow is shown in Figure 2.

(C) *Glowinski* [73]: The third effort was made by Glowinski [73] in 1984, who used a generalized framework of solving problems with discontinuities based on the theory of variational inequalities. The mathematics is more involved, use is made of Lagrange multipliers, while the solution of the corresponding minimization problem requires special Uzawa algorithms [73]. Despite the difficulty of such a formulation, solution is obtained for the ideal Bingham model, and several standard solutions have been given in the literature, which can be used for comparisons against other models [74-79].

(D) *Beris et al.* [10]: The fourth effort was made by Beris et al. [10] in 1985, who used the regularization of eq. (12), but solved for the location of the yield surface taking into account the equations for a plastic solid for  $|\dot{\gamma}| < e$ . Thus, they were able to successfully solve the benchmark problem of a sphere falling in a Bingham plastic of infinite dimensions (i.e., the boundaries of the flow domain are at infinity). In what is considered deservedly a milestone in the numerical simulation of viscoplastic fluids,

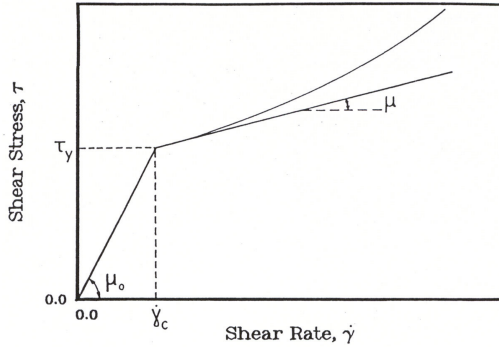


**Figure 2:** Shear stress vs. shear rate for modified Bingham and Herschel-Bulkley fluids (upper curve), according to the bi-viscosity model proposed by Tanner and Milthorpe [7] in 1983.

they found the yielded/unyielded regions, as well as the important criterion for cessation of sphere movement when a dimensionless yield stress reaches a critical value.

(E) *Papanastasiou* [26]: A fifth effort was made by *Papanastasiou* [26] in 1987, who took into account earlier works in the early 1960's (*Shangraw et al.*, [80]) as well as a well-accepted practice in the modelling of soft solids (*Gavrus et al.*, [81]), and the sigmoidal modelling behaviour of density changes across interfaces [82]. Thus, he proposed an exponential regularization of eq. (5), by introducing a parameter  $m$ , which controls the exponential growth of stress, and which has dimensions of time. The proposed model (usually called *Bingham-Papanastasiou model*) has the form (see Figure 3):

$$\bar{\tau} = \left( \mu + \frac{\tau_y}{|\dot{\gamma}|} [1 - \exp(-m|\dot{\gamma}|)] \right) \dot{\gamma} \quad \text{for all } \dot{\gamma} \quad (13)$$

and is valid for all regions, both yielded and unyielded. Thus it avoids solving explicitly for the location of the yield surface, as was done by *Beris et al.* [10].

*Papanastasiou's* modification, when applied to the different models, becomes in simple shear flow (1-D flow):

*Bingham-Papanastasiou model:*

$$\tau = \tau_y [1 - \exp(-m\dot{\gamma})] + \mu\dot{\gamma} \quad (14)$$

*Herschel-Bulkley-Papanastasiou model:*

$$\tau = \tau_y [1 - \exp(-m\dot{\gamma})] + K\dot{\gamma}^n \quad (15)$$

Casson-Papanastasiou model:

$$\sqrt{\tau} = \sqrt{\tau_y} [1 - \exp(-\sqrt{m\dot{\gamma}})] + \sqrt{\mu\dot{\gamma}} \quad (16)$$

As shown in Figure 3, the exponent  $m$  controls the stress growth, such that below the yield stress  $\tau_y$  a finite stress is allowed for vanishingly small shear rates, while the stress grows linearly with the shear rate and the viscosity  $\mu$  beyond the yield stress. Moreover, in the limit of  $m = 0$ , the Newtonian liquid is recovered, and more importantly, the limit of  $m \rightarrow \infty$  is fully equivalent to the ideal Bingham model.

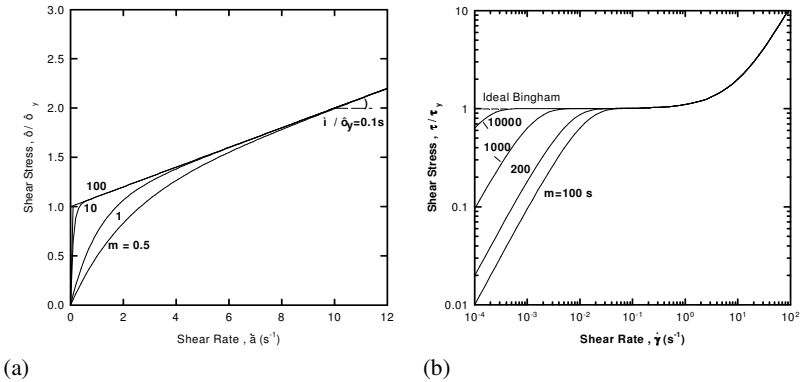


**Figure 3:** Shear stress vs. shear rate for modified Bingham fluids according to the exponential model proposed by Papanastasiou [26] in 1987 for different values of the regularization parameter  $m$ : (a) linear plot, (b) log-log plot.

Equation (14) is exact for Bingham-like viscous materials of rheological response similar to that of Figure 4, where in reality there is an apparent yield stress obtained by extrapolation from finite shear rates away from zero. In fact, because of the inability of existing measuring devices to conduct measurements at vanishingly small shear rates, where the existence of a yield stress could have been manifested, the existence of a truly Bingham fluid and the interpretation of yield stress have been questioned or reconsidered in the literature [22-25]. If such an ideal Bingham fluid does exist, in most cases it can be approximated with error comparable to that committed by finite discrete mathematics, using eq. (14) in the limit of infinitely large exponent  $m$ . The accuracy of eq. (13) has been originally checked in a variety of steady-state computations, including axisymmetric paint film formation and extrusion [26] and paint jet break-up and atomization [27].

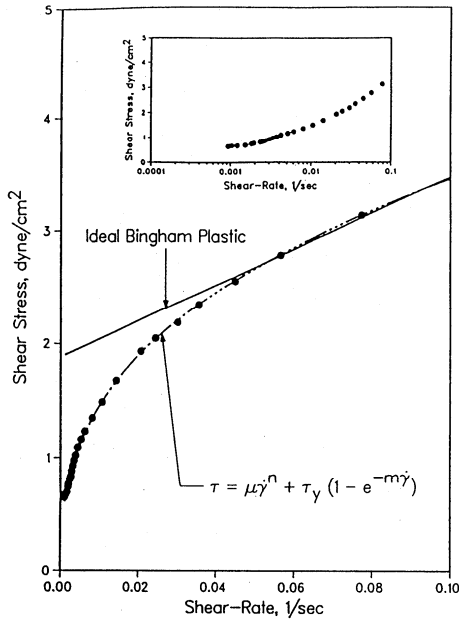


**Figure 4:** Experimental data for paint and its fit with the ideal Bingham model and the Papanastasiou modification to the Herschel-Bulkley model (from Ellwood et al., [27]).

In full tensorial form the one-dimensional constitutive equations (14-16) can be written as a purely viscous generalized Newtonian fluid:

$$\bar{\bar{\tau}} = \bar{\bar{\eta}} \bar{\bar{\dot{\gamma}}} \quad (17)$$

where  $\bar{\bar{\eta}}$  is the apparent viscosity given by:

*Bingham-Papanastasiou model:*

$$\eta = \mu + \frac{\tau_y}{|\dot{\gamma}|} [1 - \exp(-m|\dot{\gamma}|)] \quad (18)$$

*Herschel-Bulkley-Papanastasiou model:*

$$\eta = K|\dot{\gamma}|^{n-1} + \frac{\tau_y}{|\dot{\gamma}|} [1 - \exp(-m|\dot{\gamma}|)] \quad (19)$$

*Casson-Papanastasiou model:*

$$\sqrt{\eta} = \sqrt{\mu} + \sqrt{\frac{\tau_y}{|\dot{\gamma}|}} [1 - \exp(-\sqrt{m|\dot{\gamma}|})] \quad (20)$$

Tracking down yielded/unyielded regions is performed *a posteriori* by using the criterion of yield stress equal to the magnitude of the extra stress tensor  $|\tau|$ , i.e., eqs. (11).

The viscoplastic character of the flow is assessed by a dimensionless yield stress [26] or Bingham number [1] or Oldroyd number [63], defined respectively by:

$$\tau_y^* = \frac{\tau_y H}{\mu V_N} \quad (21)$$

$$Bn = Od = \frac{\tau_y D}{\mu V} \quad (22)$$

where  $H$  is a characteristic length (half the channel width or radius  $R$ ),  $D$  is the diameter or channel width ( $2H$ ),  $V_N$  is a characteristic speed taken as the average velocity of a corresponding Newtonian liquid with viscosity  $\mu$  at the same pressure gradient,  $V$  is the average velocity of the viscoplastic fluid,  $Bn$  is the Bingham number<sup>1</sup> and  $Od$  is the Oldroyd number. In all cases, the Newtonian fluid corresponds to  $\tau_y^* = Bn = Od = 0$ . However, at the other extreme of an unyielded solid,  $Bn = Od \rightarrow \infty$ , while  $\tau_y^*$  reaches a dimensionless pressure gradient having the value of 3 for Poiseuille flow in planar and 4 in axisymmetric geometries [26]. Most of the interesting viscoplastic phenomena occur in the range of  $1 < Bn < 10$ .

Using the above characteristic variables, it is possible to derive dimensionless forms of the models. Scaling the lengths by  $H$ , the velocities by  $V$ , the rates-of-strain by  $V/H$ , and the stresses and pressures by  $K(V/H)^n$ , we obtain the dimensionless stress growth exponent  $M$  as:

$$M = \frac{mV}{H} \quad (23)$$

---

<sup>1</sup> Note that a variety of symbols have been used for the Bingham number, including  $Bi$  used by Bird et al. [1], the author [28], and others [46,47]. However,  $Bi$  should be avoided as it may be confused with the Biot number of heat transfer in non-isothermal problems of viscoplastic fluids [29].

In cases where there are inertia effects (rather seldom, since viscoplastic fluids are usually very viscous materials), a Reynolds number is defined as:

$$Re = \frac{\rho V H}{\mu} \tag{24}$$

In most applications though, the Reynolds number  $Re \ll 1$ , and the creeping flow approximation to the conservation equations is valid.

The dimensionless viscosity  $\eta$  then becomes:

$$\eta = \begin{cases} 1 + \frac{Bn [1 - \exp(-M |\dot{\gamma}|)]}{|\dot{\gamma}|}, & \text{Bingham} \\ |\dot{\gamma}|^{n-1} + \frac{Bn [1 - \exp(-M |\dot{\gamma}|)]}{|\dot{\gamma}|}, & \text{Herschel - Bulkley} \\ 1 + 2 \left( \frac{Bn [1 - \exp(-\sqrt{M} |\dot{\gamma}|)]}{|\dot{\gamma}|} \right)^{1/2} + \frac{Bn [1 - \exp(-\sqrt{M} |\dot{\gamma}|)]}{|\dot{\gamma}|}, & \text{Casson} \end{cases} \tag{25}$$

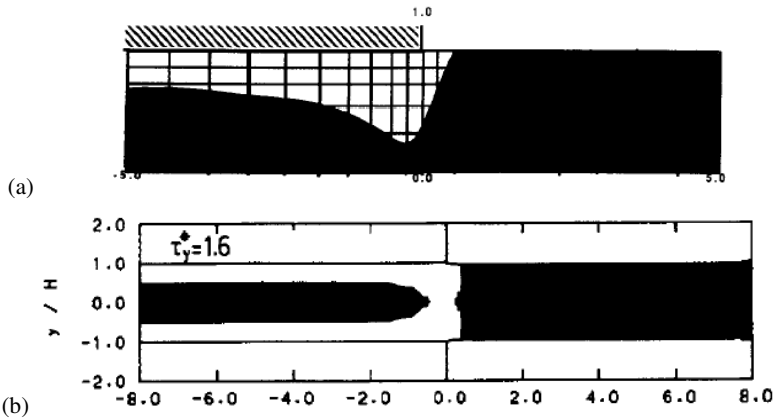


**Figure 5:** Predicted yielded (white) and unyielded (shaded black) regions in extrusion flow from a slit die of a viscoplastic fluid obeying the Bingham-Papanastasiou model with  $m=200$  s and  $\tau_y^*=1.6$ : (a) yield criterion  $|\dot{\gamma}|=0.001 \text{ s}^{-1}$ , half flow field shown [26]; (b) yield criterion  $|\dot{d}|=\tau_y^*=1.6$ , full flow field shown [28].

The dimensionless criterion for finding the yielded/unyielded regions then becomes:  $|\tau| = Bn$ . In the original work [26], the yielded/unyielded regions were found by setting an arbitrary criterion of  $|\dot{\gamma}| = 0.001 \text{ s}^{-1}$ . This led to erroneous results as shown in Figure 5a and explained by Beverly and Tanner [12]. Namely, in the problem of exit flow from a slit die, unyielded regions (shaded black) are shown at the exit, despite the fact that there is a velocity rearrangement there, and therefore the material yields. By employing the criterion of  $|\tau| = |\tau_y^*|$ , as done by Abdali et al. [28], the unyielded regions are much reduced and yielding occurs at the exit, as shown in Figure 5b. Thus, the latter criterion is more accurate and yields better results, as also argued convincingly and proven by Burgos et al. [45].

The above 5 different treatments of modelling viscoplasticity are those used in numerical simulations, while the Papanastasiou model is more and more gaining acceptance in the international computational community and is considered now the easiest and fastest way for obtaining acceptable results in flows of viscoplastic fluids. Also, the shading of the unyielded regions is considered now standard, and so they appear in a plethora of simulation works for a direct and useful visualization of the viscoplastic flow field.

### 3. METHOD OF SOLUTION

In the majority of the works, the conservation and constitutive equations, along with the appropriate boundary conditions for the problem at hand, are solved by the Finite Element Method (FEM). In our approach [28] and that of most other researchers [5-7,11,26,45-47,49-52], the primary variables are the velocities and pressure (*u-v-p* formulation). This is in contrast to the excellent work by Beris et al. [10], where the yield surface was also one of the primary unknowns. As explained in the previous papers by Abdali et al. [28,29], it is possible to get accurate results for the yielded/unyielded regions, provided many elements are used in areas of interest [77].

In our works, successive substitution (Picard iteration) is used for simplicity in the solution of the nonlinear set of equations. However, the Newton-Raphson iterative scheme has been used by others with comparable results (see, e.g., [37,38] and [49] for the squeeze flow problem). Successive solutions are obtained by using a continuation scheme, starting from the Newtonian solution and either increasing the Bingham number or the *m*-parameter in the Papanastasiou model. Because of the viscous nature of the regularized models, it is almost always possible to obtain solutions to the problem at hand, for any Bingham number, provided that continuation has been used. The number of iterations increases substantially as the plastic nature of the material becomes dominant, and one moves away from the Newtonian viscous fluid towards an elastic solid.

Streamlines are obtained *a posteriori* by solving the Poisson equation for the stream function. A plotting package is then used to draw contours of the variables, and in particular, contours of the second invariant of the stress tensor, which determine the yielded from the unyielded regions. More details can be found in the original papers [28,29,45].

#### 4. RESULTS AND DISCUSSION

In what follows, we present some representative results from several benchmark problems that have appealed to researchers in the field and have been used as standard solutions of viscoplastic flows.

##### 4.1. Entry and exit flows

The exponential modification of the Papanastasiou model has been applied to Bingham plastics to study entry and exit flows through planar and axisymmetric geometries with the purpose of determining the shape and extent of yielded/unyielded regions, extrudate swell and excess pressure losses as a function of a dimensionless yield stress or Bingham number [28].

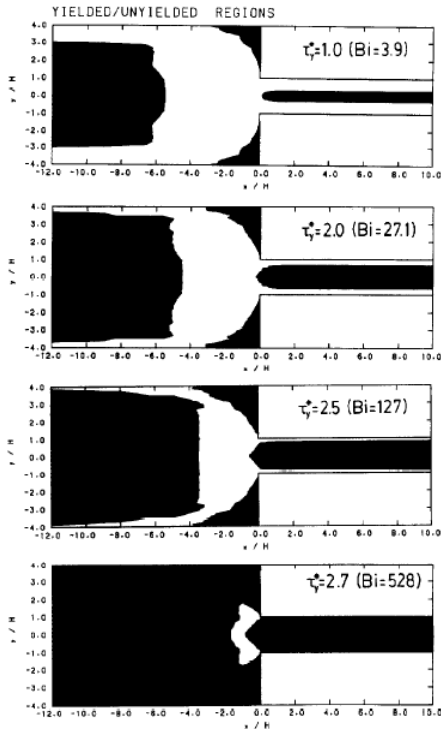


**Figure 6:** Progressive growth of the unyielded region (shaded) in entry flow through a 4:1 planar contraction of viscoplastic fluids obeying the Bingham-Papanastasiou model with  $M=200$  [28]. The flow is from left to right.

The shape and extent of yielded/unyielded regions are shown in Figure 6 for a 4:1 planar contraction. The unyielded (solid) regions are shaded solid black, while the unshaded regions correspond to deforming fluid (yielded) material. It is seen that as the Bingham number increases, the unyielded regions increase and take up the full domain, corresponding to a solid structure carried by a very thin layer of fluid on the outer perimeter of the domain (not shown for  $Bn=Bi=528$  due to pixel resolution). At the asymptotic case of  $Bi \rightarrow \infty$ , the material is all unyielded, and flow stops.

Points to notice are the two plug regions in the upstream and downstream channels, which are truly unyielded regions (TUR) and move with a plug velocity profile (no deformation), and the apparently unyielded regions (AUR) in the reservoir corners, where the velocities are very small, the area behaves as stagnant, and no deformation occurs. In reality there are very small velocities and velocity gradients, not identically zero, but the stresses there remain below the yield stress, and so the area appears as unyielded (hence shaded black).

The sharp corners appearing in the unyielded shapes of Figure 6 are due to numerical artefacts, caused basically from the use of triangular finite elements and grids not so dense, which were used at the time. Similar entry problems solved by Alexandrou and his co-workers [46,47] in flows through expansions showed smoother unyielded regions, as evidenced in Figure 7.



**Figure 7:** Progressive growth of the unyielded region (shaded) in entry flow through a 2:1 planar expansion of viscoplastic fluids obeying the Herschel-Bulkley-Papanastasiou model with  $M=1000$ ,  $n=0.5$ ,  $Re=1$  [47]. The flow is from left to right.

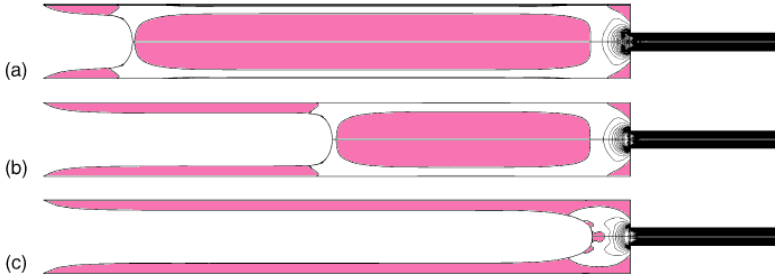


**Figure 8:** Progressive growth of the unyielded region (shaded) in transient displacement by air of viscoplastic fluids obeying the Bingham-Papanastasiou model [50]. The flow is from left to right and the fluid is displaced by air with an external pressure  $P_{ext}$ . The parameters are:  $Bn=0.05$ ,  $M=1000$ ,  $P_{ext}=5000$ ,  $Re=0$ , and the dimensionless times are: (a)  $\tau=37.5$ , (b)  $\tau=137.5$ , (c)  $\tau=200$ .

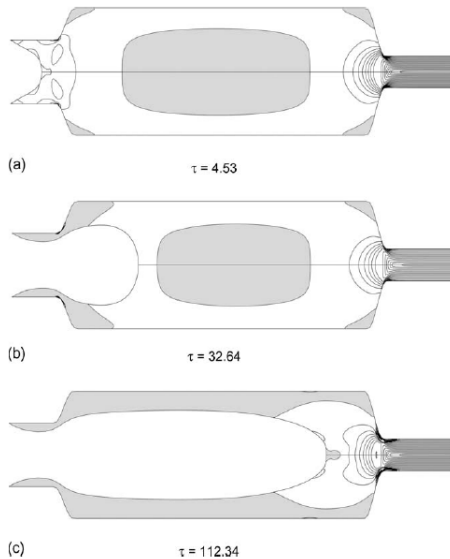


**Figure 9:** Progressive growth of the unyielded region (shaded) in transient displacement by air of viscoplastic fluids obeying the Bingham-Papanastasiou model [52]. The flow is from left to right and the fluid is displaced by air with an external pressure  $P_{ext}$ . The parameters are:  $Bn=0.04$ ,  $M=1000$ ,  $P_{ext}=50000$ ,  $Re=0$ ;  $\tau$  denotes the dimensionless time.

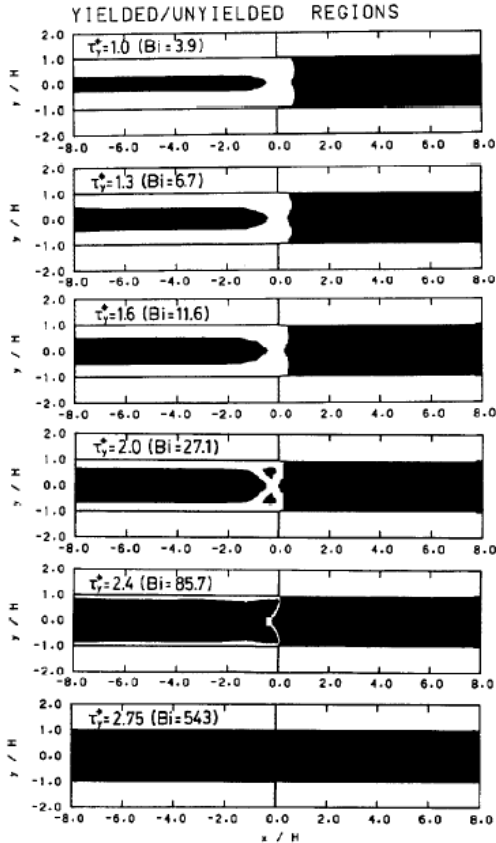


**Figure 10:** Progressive growth of the unyielded region (shaded) in exit flow through a slit die of viscoplastic fluids obeying the Bingham-Papanastasiou model with  $M=200$  [28]. The flow is from left to right.

More recently, Dimakopoulos and Tsamopoulos [50,52] have solved the gas-assisted displacement of viscoplastic fluids in a contraction [50] and in a complex tube [52] with very dense grids. In [52] they have used 36,000 triangular elements and solved in the order of 400,000 unknowns! Their transient results are shown in Figure 8 for entry flow in a contraction [50] and in Figure 9 for entry flow in a complex tube [52]. Of note is the smoothness of the results, but basically the unyielded regions (shaded) are of the same type as predicted in the early works [28,29,47]. Thus, the Papanastasiou modification to the Bingham model has given good results for many different situations of entry flows of viscoplastic fluids.

In exit flows through dies, the corresponding development of the yielded/unyielded regions is shown in Figure 10 for slit dies. As the viscoplasticity level increases (higher dimensionless yield stress or Bingham number), so the unyielded regions become bigger, and eventually those inside the die are joined together with those in the extrudate, thus forming a solid plug for very high  $Bn$  values. In all cases most of the phenomena of interest occur for  $1 < Bn < 10$ , where the viscous nature of the material competes with its plastic nature. For  $Bn < 1$ , viscous behaviour dominates, while for  $Bn > 10$ , plastic behaviour dominates the flow of these materials. Similar simulations have been also carried out for the Casson fluid [33].

The extrudate swell results are given in Figure 11 for both cases of slit and circular dies. As the viscoplasticity level increases (higher dimensionless yield stress or Bingham number), the swell decreases monotonically, reaches a minimum, after which goes asymptotically to the value of 1 (no swell, no rearrangement, all material exits as a plug). There are explanations for this non-monotonic behaviour and can be found in [28]. Similar results have been obtained recently for annular dies [44].

The excess pressure losses from the entry and exit flows give rise to the end (or Bagley) correction,  $n_B$ , which is of interest in rheometry and has been a standard way of reporting the pressure drop in a system. The end correction is a sum of the entry and exit corrections and depends as well on the contraction ratio. For viscoplastic fluids obeying the Bingham-Papanastasiou model, the corresponding results are given in Figure 12 and show a substantial linear increase with dimensionless yield stress. This has been found to obey the following empirical equations (for a 4:1 contraction) [28]:

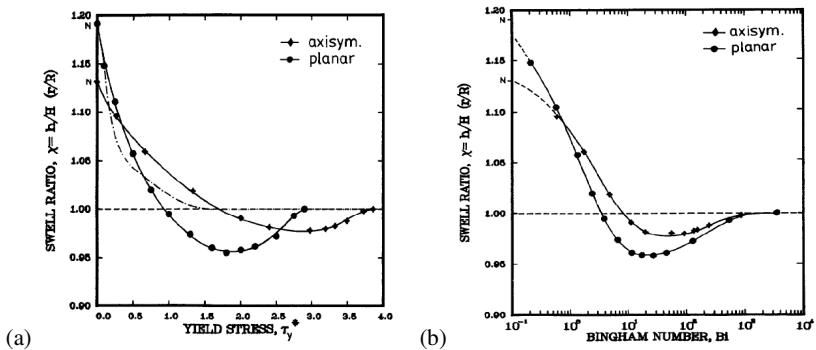


**Figure 11:** Extrudate swell for viscoplastic fluids extruded through slit and circular dies [28]: (a) swell ratio vs. dimensionless yield stress, (b) swell ratio vs. Bingham number. The fluid is obeying the Bingham-Papanastasiou model with  $M=200$ .  $N$  corresponds to Newtonian results ( $\tau_y=0$ ). The dash-dotted line corresponds to results by Papanastasiou [26] with the grid shown in Figure 5.

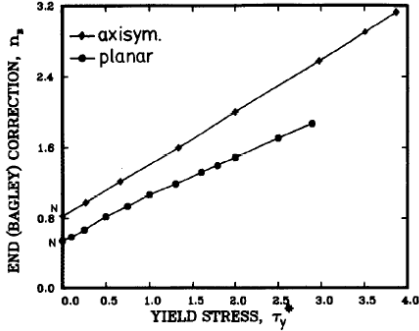


**Figure 12:** End (Bagley) correction vs. dimensionless yield stress in extrusion of viscoplastic fluids obeying the Bingham-Papanastasiou model with  $M=200$  [28].  $N$  corresponds to Newtonian result for  $\tau_y=0$ .

$$\text{(planar)} \quad n_B = 0.476\tau_y^* + 0.535 \quad \text{for } 0 \leq \tau_y^* \leq 3 \quad (26a)$$

$$\text{(axisymmetric)} \quad n_B = 0.587\tau_y^* + 0.827 \quad \text{for } 0 \leq \tau_y^* \leq 4 \quad (26b)$$

Along these lines of extrusion through dies, but a much more complicated case and an interesting problem that appeared in the literature [12] was the passage of propellant doughs, used in rocket propulsion systems, through extrusion dies. The numerical simulations using the Herschel-Bulkley-Papanastasiou model revealed the disappearance of the unyielded zones as the extrusion rate was increased from low apparent shear rates ( $1.5 \text{ s}^{-1}$ ) to very high ones ( $1200 \text{ s}^{-1}$ ) [29]. As the extrusion rate was increased, the Bingham number was reduced, and yielding became widespread. The full analysis was done under non-isothermal conditions that gave the correct temperature rise at the die exit for different extrusion rates [29]. This is an example of successfully applying a viscoplastic model to experiments and also showed the interplay of various experimental parameters to the flow behaviour of real viscoplastic materials.

#### 4.2. Flows around spheres

An important benchmark problem of fluid mechanics is flow around a sphere. The problem of a sphere falling in an infinite amount of a Newtonian fluid is the Stokes problem and has an analytical solution for the drag on the sphere, a textbook example of fluid mechanics [70,71]. The corresponding problem for a Bingham plastic does not have an analytical solution. It was solved for the first time numerically via the finite element method (FEM) by Beris et al. [10]. In this pioneering work, the yield surface was part of the solution as mentioned above. The important conclusion was that the sphere is found in the middle of a yielded region, beyond which the Bingham plastic is all unyielded and therefore does not feel any deformation. An interesting

feature of the solution was the existence of unyielded polar caps attached to the poles of the sphere, as shown schematically in Figure 13a [10].

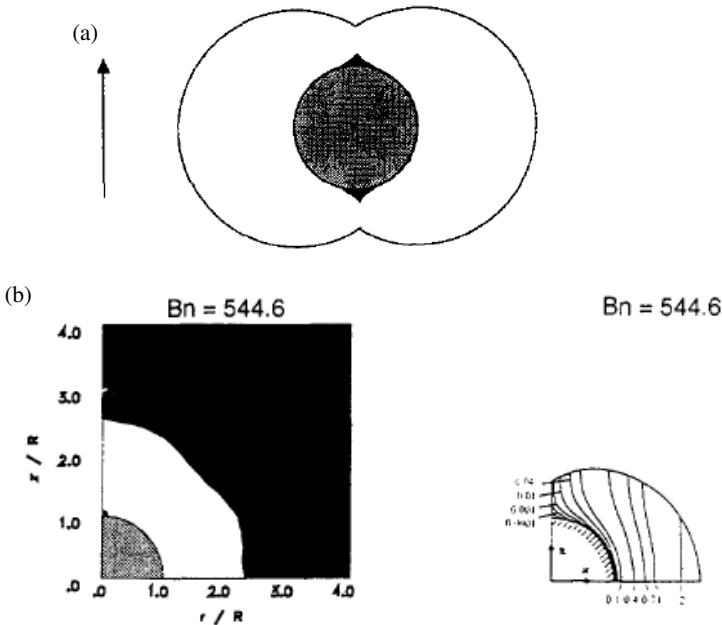


**Figure 13:** (a) Schematic representation of the shape of yielded/unyielded regions surrounding a sphere in creeping motion through an infinite Bingham medium as found by Beris et al. [10]; (b) Comparison of simulation results for a 50:1 diameter ratio (left) with the results of Beris et al. [10] for the infinite medium, regarding the extent and shape of the yielded/unyielded regions for flow of Bingham plastics around a sphere [31]. Same scale is used for the two results.

It took 12 years to revisit this problem, this time with the Bingham-Papanastasiou model and with bounding walls of a cylinder [31] instead of the infinity boundary condition used by Beris et al. [10]. The results were surprisingly close, as evidenced in Figure 13b for the same  $Bn$  number. Even the polar caps were well captured by the continuous model with no extra effort. The major difference was in the flow ( $z$ -) direction, where the Bingham-plastic results showed an indentation not found with the continuous model. It is not clear whether this is an influence of the presence of the bounding walls. The walls do have an influence, as shown in the development of the yielded/unyielded regions in Figure 14 for an 8:1 diameter ratio ( $=R_c/R$ , where  $R_c$  is the radius of the containing cylinder and  $R$  the sphere radius).

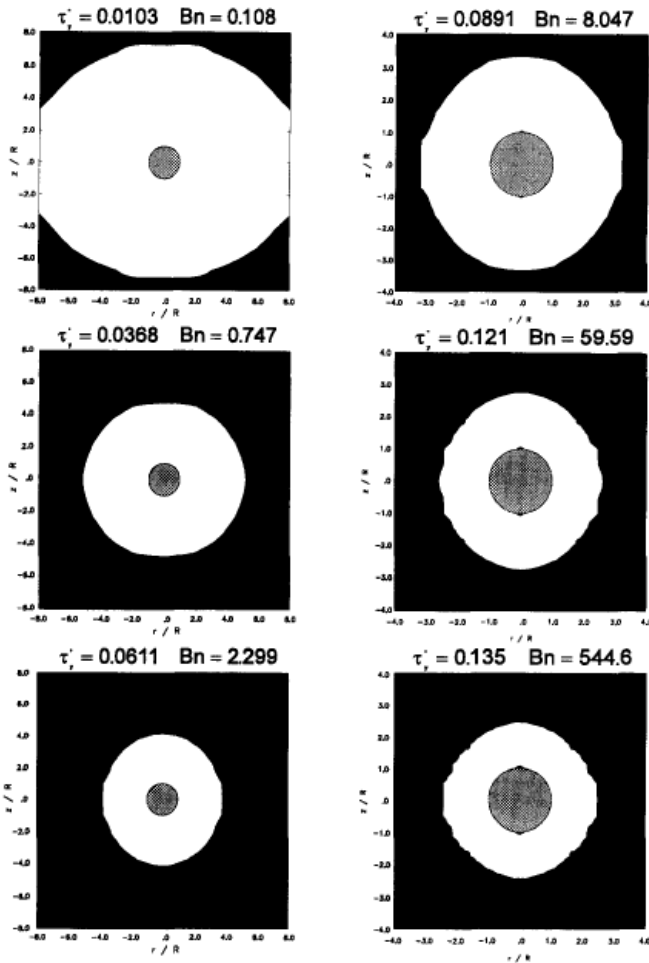


**Figure 14:** Progressive growth of the unyielded region (shaded) for flow of viscoplastic fluids obeying the Bingham-Papanastasiou model around a sphere contained in a tube with an 8:1 diameter ratio [31]. The RHS column is zoomed around the sphere.

As the  $Bn$  number increases, the unyielded regions come closer to the sphere but they always leave a considerable space around it where yielding occurs, even at the highest  $Bn=6,000,000$  for which calculations were performed [31].

The results for the drag are presented in Figure 15 and show another interesting feature of this benchmark problem. Namely, a key limiting value of the dimensionless yield stress  $\tau_y^* = 0.143$ , beyond which the sphere will cease to move. This value was found by Beris et al. [10] by extrapolation and some analytical handling of their numerical results, and may hold for all objects, where the radius  $R$  is replaced by the hydraulic radius  $R_h$  of the object in question. This postulate needs further research.

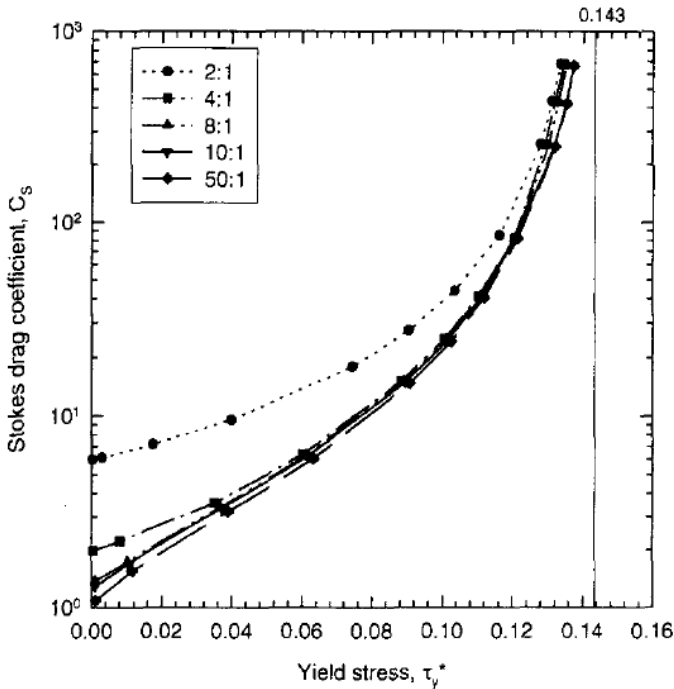


**Figure 15:** Drag coefficient vs. dimensionless yield stress for Bingham plastics flowing around a sphere contained in a tube for different diameter ratios. The value of 0.143 corresponds to the infinite case [10] and represents the ultimate value of dimensionless yield stress beyond which the sphere will not fall [31].

This benchmark problem has been given special attention in the experimental community because of its simplicity and apparent ease of measuring the drag force on the sphere. Thus, Atapattu et al. [55,56] performed the relevant experiments and were able to also determine experimentally the yielded/unyielded regions for spheres falling in various viscoplastic Herschel-Bulkley fluids. The corresponding simulations were performed by Beaulne and Mitsoulis [32] and showed a remarkable agreement with

the experiments as evidenced in Figure 16. Also the drag on the sphere was well predicted, so that this appears to be a well-understood and solved problem.

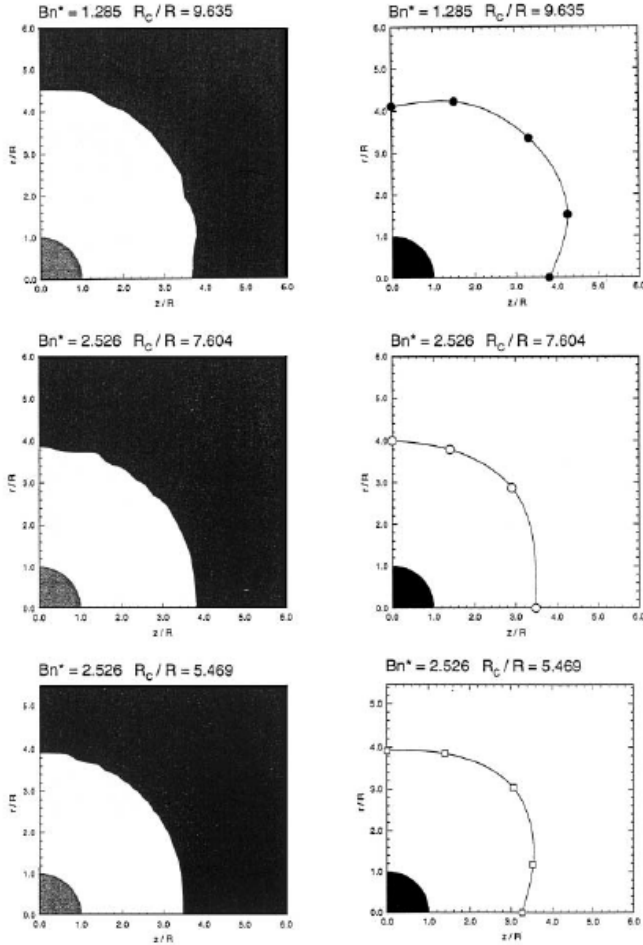


**Figure 16:** Comparison of simulation results [32] (left column) with the results of Atapattu et al. [56], regarding the extent and shape of the yielded/unyielded regions for flow of a Herschel-Bulkley fluid around a sphere. The simulations were performed with the Herschel-Bulkley-Papanastasiou model with  $M = 1000$ .

### 4.3. Flows around cylinders

Another benchmark problem that has been dealt with by the scientific community from the early years of analytical [83] or approximate solutions [84] is the flow around a cylinder. There are two variations of this flow: (a) pressure-driven flow around a cylinder, and (b) drag flow around a cylinder. Faxen [83] has given the analytical expressions for Newtonian fluids in either case, while for the drag case Adachi and Yoshioka [84] have found through variational principles the extent and shape of yielded/unyielded regions and the drag on the cylinder in the extreme cases of maximum and minimum integrations (see Figure 17b and 17c).

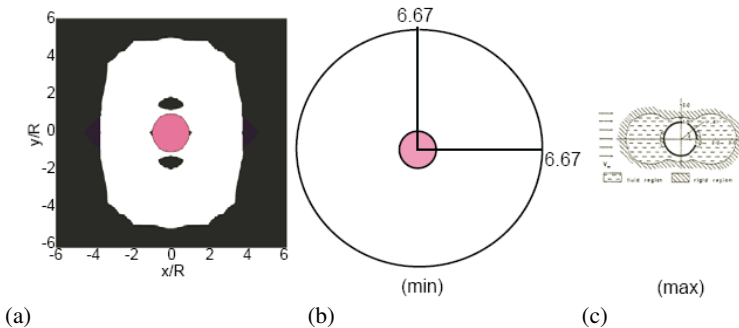


**Figure 17:** Drag flow past a cylinder, regarding the extent and shape of the yielded/unyielded regions for  $Bn=10$ : (a) simulation results for  $H/R=50$  with the Bingham-Papanastasiou model with  $M=1000$  [39], (b) variational minimum integral results for  $H/R=\infty$  [84], (c) variational maximum integral results for  $H/R=\infty$  [84]. The flow is from left to right. Graphs are drawn in scale.

The drag flow problem was solved with the regularized Papanastasiou model by several authors with comparable results [39,77,85]. The yielded/unyielded regions predicted by the simulations (Figure 17a) are between the maximum and minimum variational predictions of Adachi and Yoshioka [84] as expected. In the comparison simulations, a 50:1 gap/diameter ratio ( $=H/R$ , where  $H$  is the half gap between the parallel plates and  $R$  the cylinder radius) has been used while the variational results are valid for  $H/R=\infty$ .

The usual development of the yielded/unyielded regions is shown in Figure 18 for the case of  $H/R=2$  as the dimensionless yield stress or Bingham number increases. Because of the drag flow (plug velocity imposed away from the cylinder and on the parallel plates), all regions before and after the cylinder are unyielded, and yielding occurs near the cylinder.

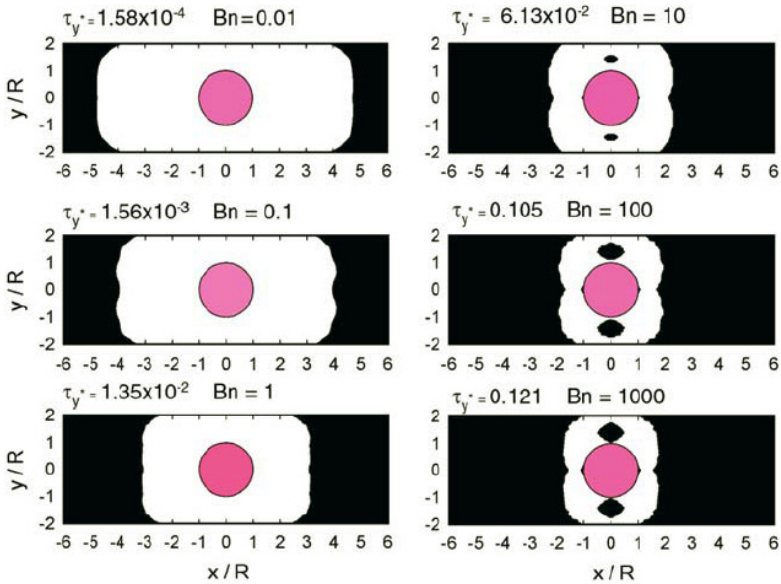
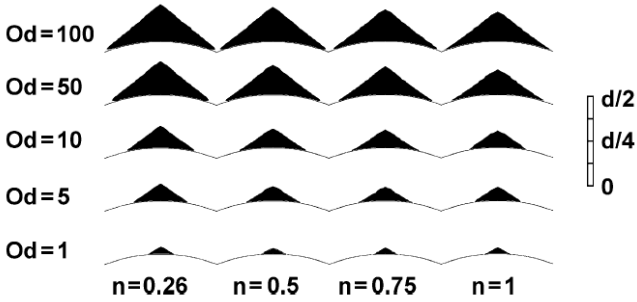


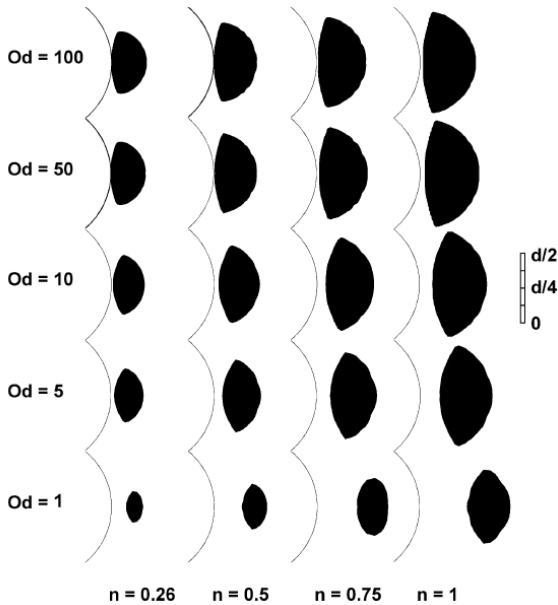
**Figure 18:** Progressive growth of the unyielded region (shaded) for drag flow of viscoplastic fluids obeying the Bingham-Papanastasiou model with  $M=1000$  around a cylinder contained between parallel plates with gap/diameter ratio  $H/R=2$  [39]. Flow is from left to right.

Another feature of this problem is the appearance of caps around the stagnation points of the cylinders (poles) and also (surprisingly) the appearance of islands above and below the cylinder (the equator). These unyielded (rigid) zones, shown in magnification in Figure 19 from simulations with the Herschel-Bulkley-Papanastasiou model [85], have been borne out by all simulations [39,77,85] and appear to be a special feature of this problem and the planar geometry, which always shows bigger unyielded regions than a corresponding axisymmetric geometry.

The drag on the cylinder is shown in Figure 20 and appears to obey the limiting dimensionless yield stress value of 0.143, beyond which flow ceases. Again it is not clear whether this value found for spheres is valid for cylinders as well, although it appears to be a good postulate, when the sphere radius  $R$  is substituted by the hydraulic radius  $R_h$  for other objects.



(a)



(b)

**Figure 19:** Special unyielded (rigid) regions in drag flow past a cylinder of diameter  $d$  for different Oldroyd numbers ( $Od$ ) and power-law indices  $n$ . Simulation results for  $H/R=15$  with the Herschel-Bulkley-Papanastasiou model with  $M=10^4/Od$  [85]: (a) rigid regions (caps) attached to the stagnation points (poles), (b) rigid regions appearing as islands on either side of the cylinder (equator). The flow is from bottom to top.

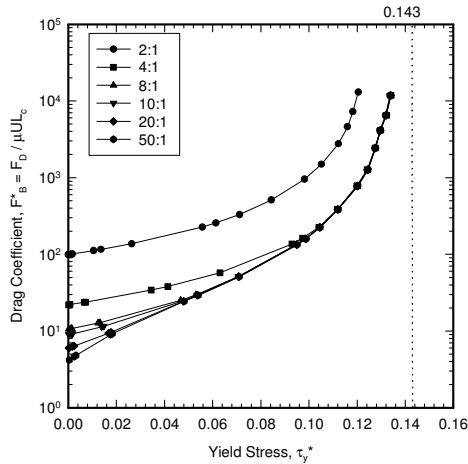


**Figure 20:** Drag coefficient vs. dimensionless yield stress for Bingham plastics in drag flow around a cylinder contained between parallel plates for different gap/diameter ratios  $H/R$ . The cylinder has length  $L_c$  and is dragged with a velocity  $U$ . The value of 0.143 corresponds to the infinite case [10] and represents the ultimate value of dimensionless yield stress beyond which a *sphere* will not fall.

#### 4.4. Squeeze flows

The squeeze flow problem owes its appeal to a simple rheometry test for measuring the yield stress of viscoplastic materials. This takes place in a plastometer [14], which is a simple device of squeezing a sample between two disks or parallel plates. Because of this simplicity, the squeeze flow problem has attracted a very considerable attention both experimentally and theoretically, including simplified analysis [86,87,88] and complicated simulations [89]. As mentioned above, an excellent recent review article by Engmann et al. [66] encompasses most of the works up to 2005 and highlights outstanding problems and questions still remaining in this rich subject.

From a simulation point of view, early works on viscoplastic fluids saw the tackling of this problem as well [8,9]. As shown in Figure 21, there was a controversy regarding the location of yielded/unyielded regions, with Covey and Stanmore [14] assuming that the location of the unyielded regions was in the middle of the flow field (Figure 21a). The first to correctly calculate the unyielded regions were O'Donovan and Tanner [9], who showed them to be just around the stagnation points in the middle of the disks and attached to them. Recent work by Smyrniotis and Tsamopoulos [49] and the author [37,38] verified this finding, as shown in Figure 21b. All these works assume a quasi-steady-state flow and have solved for different aspect ratios  $\varepsilon=H/R$ .

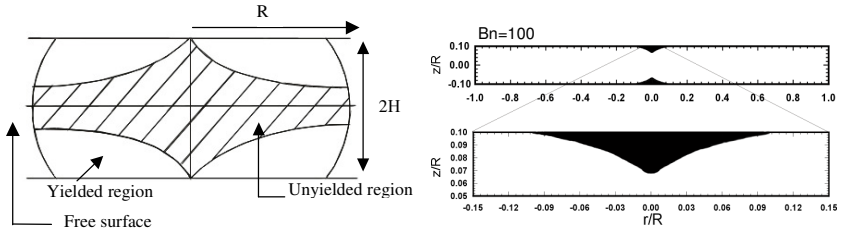


**Figure 21:** Squeeze flow in a plastometer: (a) assumed yielded / unyielded regions according to Covey and Stanmore [14], (b) calculated unyielded regions (shaded black) for aspect ratio  $\varepsilon=0.1$  and  $Bn=100$  [9,37,38,49].

The dependence of squeeze force on aspect ratio  $\varepsilon$  for different  $Bn$  numbers and for both geometries is shown in Figure 22 [38]. Omitting the free surface at the edges of the sample reduces the squeeze force by at most 2%.

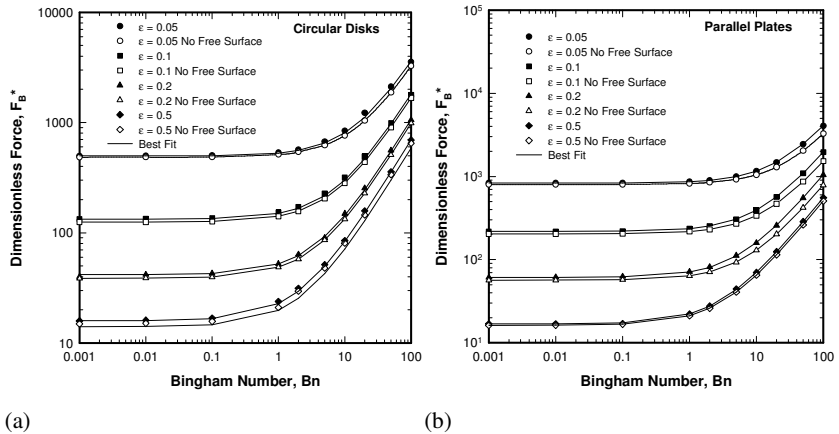


**Figure 22:** Squeeze force in a plastometer: (a) circular disks, (b) parallel plates [38].

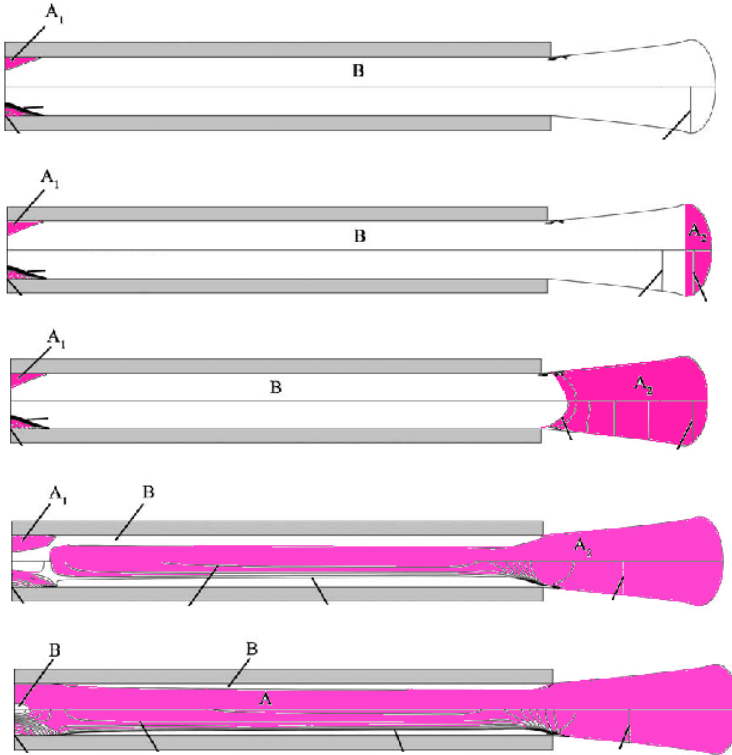


**Figure 23:** Yielded (B) / unyielded (A, shaded) regions in transient squeeze flow of viscoplastic fluids obeying the Bingham-Papanastasiou model [51]. The conditions are for  $Bn=10$ ,  $M=500$ ,  $\varepsilon=0.1$ ,  $w=10$ ,  $Re=0$ . Flow under a constant squeeze force for different times with time increasing from top to bottom. The dimensionless times are: 5.03, 5.21, 6.49, 13.06, 17.16. Due to radial symmetry, half the domain is shown.

The lines are best fitted by the following equation:

$$(Axisymmetric\ geometry) \quad F_B^* = \frac{1.867}{\varepsilon^{1.862}} (1 + 1.649 Bn \varepsilon^{1.096}), \quad (0.01 \leq \varepsilon \leq 0.1), \quad (27a)$$

The corresponding planar results are best fitted by the following equation:

$$(Planar\ geometry) \quad F_B^* = \frac{2.327}{\varepsilon^{1.96}} (1 + 1.046 Bn \varepsilon^{1.098}), \quad (0.01 \leq \varepsilon \leq 0.1), \quad (27b)$$

Both formulas have a maximum absolute error of 10-11% in the range of applicability.

The results from transient simulations for a constant squeeze force have also been recently obtained by Karapetsas and Tsamopoulos [51] for a variation of the process, where the material is allowed to move beyond the edges of the disks. Very interesting free surfaces and yielded/unyielded regions were found with the Bingham-Papanastasiou model, as shown in Figure 23 for different dimensionless time instants. The parameters are for creeping flow conditions ( $Re=0$ ) with  $Bn=10$ ,  $M=500$ ,  $\varepsilon=0.1$ ,  $w=10$ , where  $\varepsilon=H/r$  is the initial aspect ratio ( $r < R$ ) and  $w=R/H$  is the initial material aspect ratio, since the material initially does not extend to the edge of the disk. The squeeze force, appropriately calculated to correspond to the quasi-steady-state simulations, i.e., for different  $\varepsilon$ , was not found to be very different from the results given in Figure 22. This is not surprising, since the force is an integral quantity, which depends mainly on the geometry and the Bingham number, as given by eqs. (27).

#### 4.5. Flows in processing units

Apart from the above benchmark problems, where the various viscoplastic models have been tested and standard solutions have been obtained, there are also the more industrially important viscoplastic materials processing through various types of equipment. A major industry interested in viscoplastic materials is the food processing industry, since many foodstuff exhibit a yield stress [1]. Also, ceramic slurries are routinely coated on substrates for semiconductor and other applications [30]. Mud-drilling is another operation requiring equipment, usually of concentric or eccentric annuli, hence the many papers dealing with the subject [90-92]. Also, in biomedical engineering, blood flow is a major concern inside the human body [93], with blood usually assumed to obey the Casson model [33].

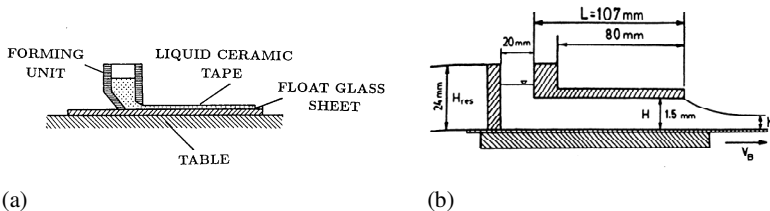


**Figure 24:** (a) Blade coating of a ceramic slurry. The material flows under gravity and is dragged by a moving substrate (float glass sheet) to be coated on the moving web, while the tip of the blade (right wall of the reservoir) also helps determine the final coating thickness; (b) dimensions of a typical unit [30].

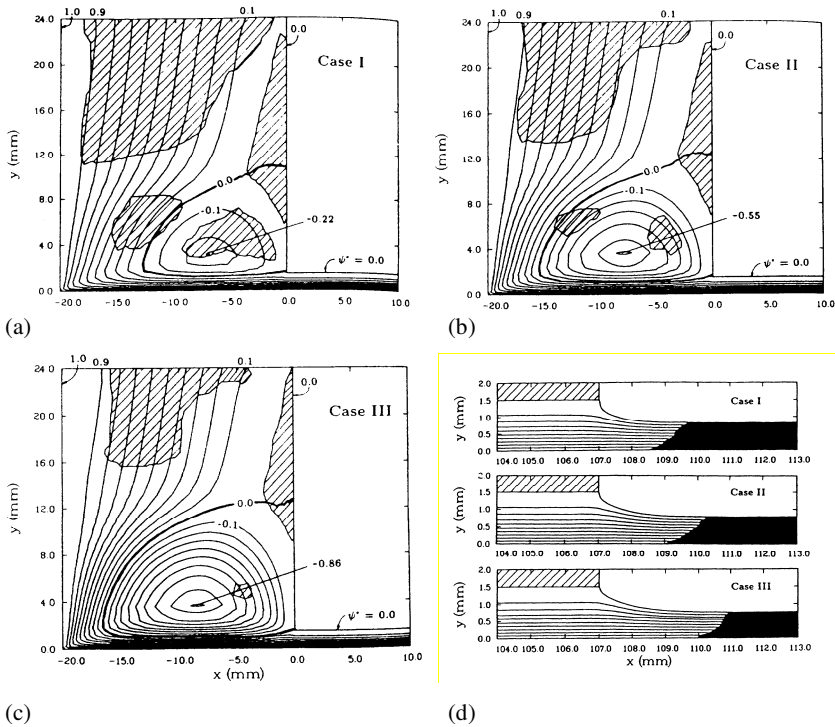


**Figure 25:** Yielded / unyielded (shaded) regions in blade coating of a ceramic slurry obeying the Bingham-Papanastasiou model with  $m=200$  s [30]: (a) flow in the reservoir for  $V_B=3.79$  mm/s, (b) flow in the reservoir for  $V_B=7.58$  mm/s, (c) flow in the reservoir for  $V_B=15.16$  mm/s, (d) exit flow on the substrate for the 3 different web speeds  $V_B$  [30].

From the many processes, which have been analyzed with viscoplastic materials, some typical examples will be given here. These are: (a) blade coating, (b) wire coating, (c) calendering.

#### 4.5.1. Blade coating

Ceramic slurries are coated on substrates by the blade coating process for semiconductor and other applications (see Figure 24). A proper design must coat the material with a smooth surface and a homogeneous coating at increasingly higher substrate speeds.

Calculations have been carried out at different substrate speeds  $V_B$  for a ceramic slurry that behaved as a Bingham plastic [30]. Figure 25 reveals the extent and shape

of the yielded/unyielded regions for 3 different increasing speeds (cases I, II and III). It is seen that by increasing the substrate speed, the recirculation increases in the reservoir, the unyielded (shaded) regions decrease, while after the blade exit the unyielded regions move farther away from the exit (Figure 25d). These simulations were used to verify experimental data [94] and to deduce a new design for the casting unit (Figure 26) that would eliminate recirculation and reduce the undesirable unyielded regions [30]. Basically the new design consists of tapering the left reservoir wall to bring it closer to the tip of the blade, so that there is not enough space in the reservoir for a vortex to form. The analysis can be easily done by the 1-dimensional Lubrication Approximation Theory (LAT), which gives the necessary height for no back flow in a drag flow situation. Such an analysis was originally used by Caswell and Tanner [95] in the wire-coating process.

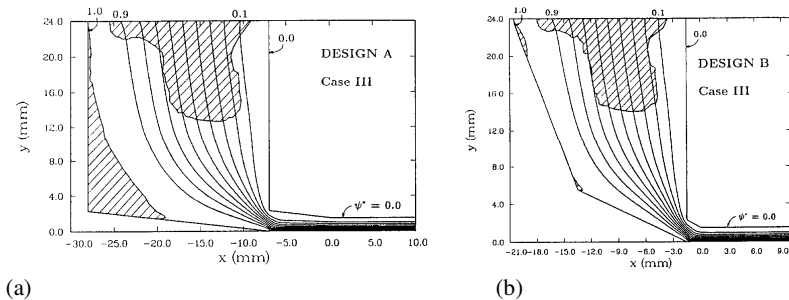


**Figure 26:** New designs for blade coating of a viscoplactic ceramic slurry: (a) Design A eliminates the vortex but still leaves big unyielded areas (shaded) near the left wall of the reservoir, while (b) Design B eliminates both the vortex and these unyielded areas for a better streamlined flow in the unit [30].

#### 4.5.2. Wire coating

One of the important forming processes, especially in the plastics industry, is the wire-coating process, in which, a moving bare wire passes through an extruder die head and is coated by a polymer melt supplied under pressure from the extruder (see Figure 27a) [96]. The coating process takes place in minute volumes, and only through numerical simulation can one study the flow behaviour inside wire-coating dies. On the other hand, the industrial design of wire-coating dies (Figure 27b) is based on empiricism to guarantee a smooth streamlined flow of the material being coated [97].



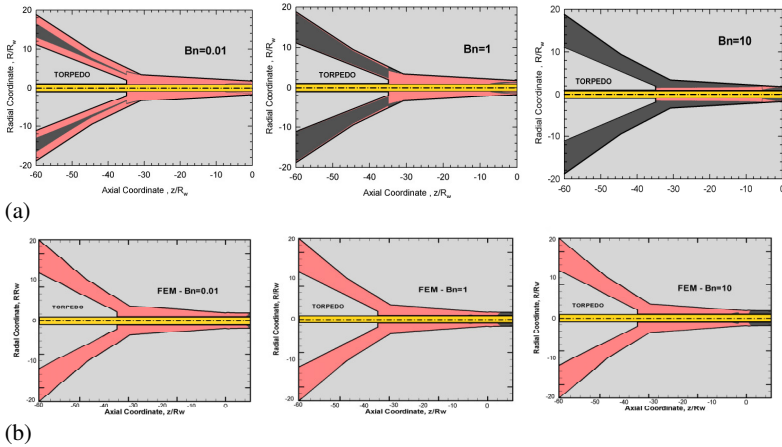


**Figure 28:** (a) Yielded/unyielded (black) regions in wire coating of viscoplastic fluids obeying the Bingham model according to LAT; (b) yielded/unyielded (black) regions in wire coating of viscoplastic fluids obeying the Bingham-Papanastasiou model with  $m=1000$  s, according to a fully 2-D FEM simulation [99]. The flow is from left to right in the die design of Figure 27b.

It is only after the die exit where unyielded regions appear. There a plug velocity profile exists, due to the movement of the coating fluid as a solid plug on the moving wire. An increase of the Bn number brings the solid plug closer to the die exit (towards  $z = 0$ ). However, the pressure distribution and the ensuing operating variables were within 10% (in the range  $0 \leq Bn \leq 1000$ ) of the values found by LAT, as was the case for pseudoplastic fluids.

It is therefore obvious that the introduction of LAT in lubrication flows with viscoplastic fluids is not valid for such quantities as the yielded/unyielded regions, since it leads to a “paradox”, as pointed out by Lipscomb and Denn [100]. A 2-D analysis is therefore essential in obtaining the correct regions. However, it does not change drastically the other results, especially the pressure distribution and integrated quantities, since wire coating is primarily a lubrication flow. The FEM 2-D calculations confirmed this.

### 4.5.3. Calendering

The calendering process is used in a wide variety of industries for the production of rolled sheets or films of specific thickness and final appearance. It involves a pair of co-rotating heated rolls (calenders) which are fed with a material to form a sheet of specific thickness. There are two variants of the process: a feed from an infinite reservoir (Figure 29a) and a feed with a finite sheet (Figure 29b) [101].

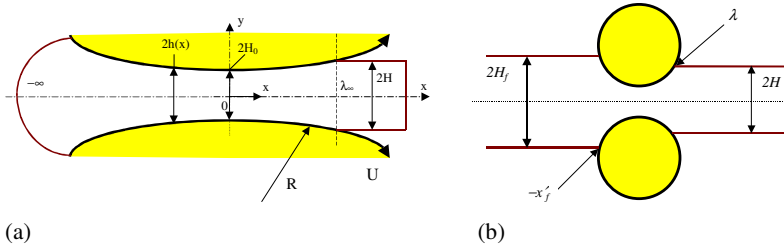


**Figure 29:** Schematic representation of the calendaring process between two co-rotating rolls [101]: (a) feed from an infinite reservoir, (b) feed with a finite sheet to produce a final sheet thickness of  $2H$ .

The analysis of the process for viscoplastic materials was first performed by Gaskell [102], who used LAT to deduce the yielded/unyielded regions. Interesting patterns were found, as shown in Figure 30 and verified by Chung [103] using LAT. Basically, LAT predicts sheared unyielded regions close to the rolls, while the rest of the material flows as unyielded. Higher values of the yield stress reduce the yielded regions, as expected (Figure 30b).

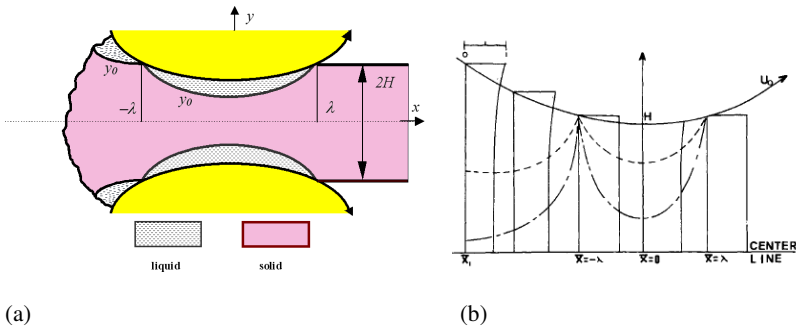


**Figure 30:** (a) Schematic representation of yielded / unyielded regions in calendaring according to Gaskell [102] based on LAT with an infinite reservoir; (b) calculated yielded/unyielded regions according to Chung [103] based on LAT with a finite sheet. The dashed line is for a higher yield stress, while the dash-dotted line is for a lower yield stress. The flow is from left to right and not in scale.

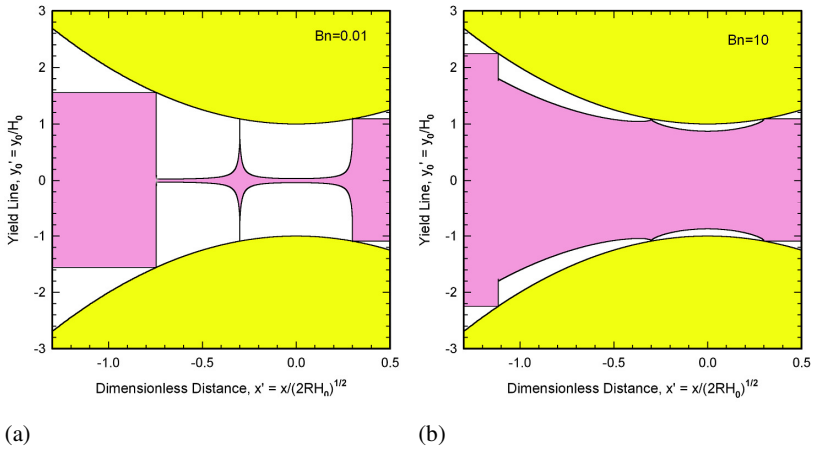


**Figure 31:** Calculated yielded / unyielded (shaded) regions in calendaring of viscoplastic fluids obeying the Bingham model according to LAT for a feed with a finite sheet [104]: (a)  $Bn=0.01$  and (b)  $Bn=10$ . The flow is from left to right and not in scale.

A full and detailed parametric study of viscoplastic fluids for different Bingham numbers employing the Bingham and the Herschel-Bulkley models has been performed by Sofou and Mitsoulis [104] for a finite feed. Sample results are shown in Figure 31 for a low  $Bn=0.01$  and a high  $Bn=10$  and for a dimensionless exit distance  $\lambda=0.3$ . These results corroborate the previous findings based on LAT, and provide detailed calculations for the pressure, force, torque and power input in calendaring. Another work [105] deals with a feed from an infinite reservoir, while the effect of slip at the wall is examined in [106].

However, as explained above for the case of wire coating, while LAT gives good results for the pressure and all engineering quantities ensuing from it, it grossly miscalculates the yielded/unyielded regions. Fully 2-D FEM results based on the Bingham-Papanastasiou model for the conditions of Figure 31 are presented in Figure 32 and show the greatly reduced unyielded regions in calendaring of viscoplastic materials [107]. Thus, it is again demonstrated that although LAT gives fast results, which are good for engineering calculations, it gives erroneous results for the location of the yielded/unyielded regions as pointed out by Lipscomb and Denn [100]. When these regions are of interest, a fully 2-D or 3-D analysis becomes necessary for all flow fields, even those that can be approximated as lubrication flows.

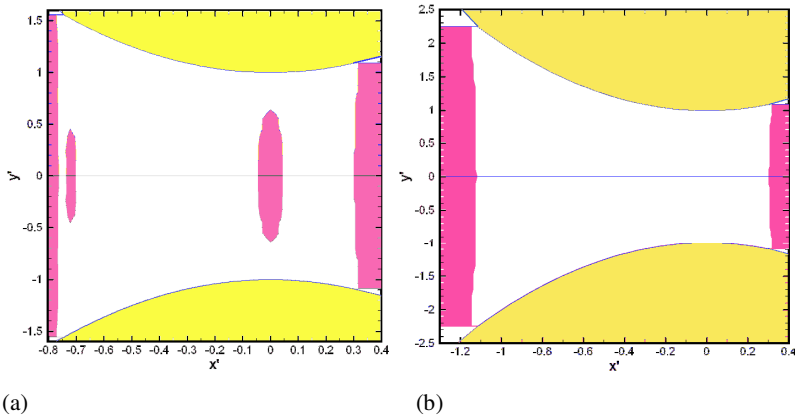


**Figure 32:** Calculated yielded / unyielded (shaded) regions in calendaring of viscoplastic fluids obeying the Bingham-Papanastasiou model with  $m=1000$  s, according to a fully 2-D FEM simulation for a feed with a finite sheet [107]: (a)  $Bn=0.01$  and (b)  $Bn=10$ . The flow is from left to right and not in scale.

## 5. CONCLUSIONS

In this review, the flow of viscoplastic materials exhibiting a yield stress has been discussed with the emphasis on the models and computations that have appeared in the last 25 years or so. More specifically, the original discontinuous models of viscoplasticity have been presented together with their modifications to make them amenable to numerical simulations in non-trivial flows. From these models, the exponential modification of Papanastasiou has shown attractive properties and has dominated the simulations both for benchmark problems and for processing flows by a variety of researchers. Its convergence behaviour, being essentially that of a generalized Newtonian model, is easy and good, either with a Picard or with a Newton-Raphson iterative scheme, provided that continuation is used from the linear Newtonian limit to the highly nonlinear plastic limit.

Because of its simplicity and ease of use, the Papanastasiou model has been included in most (if not all) of the commercial fluid-flow software available, and has been used to solve benchmark problems, some of which have been summarized in this work. These include entry and exit flows from dies, flows around spheres and cylinders, and the squeeze flow problem that is relevant in plastometry for the determination of yield stress. The problems are usually solved as parametric studies in the range of  $Bn$  numbers from 0 (viscous limit) to infinity (plastic limit). Most of the

interesting viscoplastic phenomena occur for  $1 < Bn < 10$ . These test problems have shown the extent and shape of the yielded/unyielded regions due to the existence of the yield stress. Although the accuracy of these regions depends somewhat on the mesh density used and the regularization parameter of the Papanastasiou model (the stress growth exponent), they all basically agree in the main features of the unyielded regions. These regions are now routinely shaded dark (or black) in the simulations for easy identification of the zones of no deformation.

The Papanastasiou model has also been used in processing flows of viscoplastic materials, which are of great interest in many industries, such as in food processing, in semiconductor processing, in the petroleum industry for drilling operations, in the semisolid processing industry [108], to name just a few. Although very few 3-D problems have appeared in the open literature, it is quite probable that the model is used routinely for complicated 3-D die design in many R&D departments, the results of which are of course of proprietary nature. Nevertheless, there are benchmark 3-D flows, where simulation results are still missing, as in viscoplastic flows around objects [61]. Although there are in principle no difficulties in applying the continuous model in 3-D simulations, this largely remains to be done in the open literature. The same is also true for time-dependent simulations, which have just recently been undertaken [41,42,50-52].

A natural sequence of modelling viscoplasticity is the modelling of thixotropy [109], a more demanding subject, since it involves time-dependence and structure in addition to the existence of a yield stress. The subject of structure development and destruction in thixotropic or rheopectic fluids is very interesting and apparently rather difficult [110]. A literature survey reveals few successful modelling and simulation efforts. Having resolved most of the issues of handling simple viscoplasticity with the continuous regularized models, it is now possible to add the necessary structure parameters to handle more complicated situations as these arise in many real industrial applications of thixotropic materials [111]. This recent work tries to incorporate more realistic features to bridge the gap between the simple viscoplastic model of Herschel-Bulkley and structure of semisolid suspensions. Such commercial materials typically consist of viscoplastic components and are processed in rather complex flow fields. Although no complete picture has emerged so far, it is encouraging to observe that a significant effort is put into the quest of mechanistically understanding the individual phenomena, rather than focusing on the combination of all effects. It is our belief that, in the long run, such an approach will lead to a scientifically based design approach for materials, optimally structured at the appropriate scale that is necessary to tailor their property profile.

## ACKNOWLEDGEMENTS

The author is indebted to many colleagues with whom he held discussions over the last 20 years about viscoplastic fluids, among them Profs. T.C. Papanastasiou, J.-M. Piau, R.R. Huilgol, A.N. Alexandrou, G.C. Georgiou and J.A. Tsamopoulos.

## REFERENCES

1. Bird, R.B., Dai, G.C., Yarusso, B.J., *The rheology and flow of viscoplastic materials*, Rev. Chem. Eng., 1 (1983) 1-70.
2. Bingham, E.C., *Fluidity and plasticity*, McGraw-Hill, New York (1922).
3. Herschel, W.H., Bulkley, R., *Konsistenzmessungen von Gummi-Benzol-Lösungen*, Kolloid Z., 39 (1926) 291-300.
4. Casson, N., *Rheology of disperse systems*, Ed. C.C. Mill, Pergamon Press, Oxford (1959).
5. Bercovier, M., Engelman, M., *A finite-element method for incompressible non-Newtonian flows*, J. Comput. Phys., 36 (1980) 313-326.
6. Gartling, D.K., *The numerical simulation of plastic fluids*, Num. Meth. Lam. Turb. Flow (Eds. C. Taylor, J.A. Johnson, W.R. Smith), Proc. 3rd Int. Conf., Seattle, Pineridge Press, Swansea, 669-679 (1983).
7. Tanner, R.I., Milthorpe, J.F., *Numerical simulation of the flow of fluids with yield stress*, Num. Meth. Lam. Turb. Flow (Eds. Taylor, C., Johnson, J.A., Smith, W.R.), Proc. 3rd Int. Conf., Seattle, Pineridge Press, Swansea (1983) 680-690.
8. Gartling, D.K., Phan-Thien, N., *A numerical simulation of a plastic fluid in a parallel-plate plastometer*, J. Non-Newtonian Fluid Mech., 14 (1984) 347-360.
9. O'Donovan, E.J., Tanner, R.I., *Numerical study of the Bingham squeeze film problem*, J. Non-Newtonian Fluid Mech., 15 (1984) 75-83.
10. Beris, A.N., Tsamopoulos, J.A., Armstrong, R.C., Brown, R.A., *Creeping motion of a sphere through a Bingham plastic*, J. Fluid Mech., 158 (1985) 219-244.
11. Scott, P.S., Mirza, F., Vlachopoulos, J., *Finite-element simulation of laminar viscoplastic flows with regions of recirculation*, J. Rheol., 32 (1988) 387-400.
12. Beverly, C.R., Tanner, R.I., *Numerical analysis of extrudate swell in viscoelastic materials with yield stress*, J. Rheol., 33 (1989) 989-1009.
13. Beverly, C.R., Tanner, R.I., *Numerical analysis of three-dimensional Bingham plastic flow*, J. Non-Newtonian Fluid Mech., 42 (1992) 85-115.
14. Covey, G.H., Stanmore, B.R., *Use of the parallel-plate plastometer for the characterisation of viscous fluids with a yield stress*, J. Non-Newtonian Fluid Mech., 8 (1981) 249-260.
15. Keentok, M., Milthorpe, J.F., O'Donovan, E.J., *On the shearing zone around rotating vanes in plastic liquids: theory and experiment*, J. Non-Newtonian Fluid Mech., 17 (1985) 23-35.
16. Dzuy, N.Q., Boger, D.V., *Yield stress measurement for concentrated suspensions*, J. Rheol., 27 (1983) 321-349.

17. Dzuy, N.Q., Boger, D.V., *Direct yield stress measurement with the vane method*, J. Rheol., 29 (1985) 335-347.
18. Nguyen, Q.D., Boger, D.V., *Characterization of yield stress fluids with concentric cylinder viscometers*, Rheol. Acta, 26 (1987) 508-515.
19. Magnin, A., Piau, J.M., *Shear rheometry of fluids with a yield stress*, J. Non-Newtonian Fluid Mech., 24 (1987) 91-106.
20. Magnin, A., Piau, J.M., *Cone-and-plate rheometry of yield stress fluids. Study of an aqueous gel*, J. Non-Newtonian Fluid Mech., 36 (1990) 85-108.
21. Nguyen, Q.D., Boger, D.V., *Measuring the flow properties of yield stress fluids*, Annu. Rev. Fluid Mech., 24 (1992) 47-88.
22. Barnes, H.A., Walters, K., *The yield stress myth*, Rheol. Acta, 24 (1985) 323-326.
23. Harnett, J.P., Hu, R.Y.Z., *The yield stress – an engineering reality*, J. Rheol., 33 (1989) 671-679.
24. Schurz, J., *The yield stress - an empirical reality*, Rheol. Acta, 29 (1990) 170-171.
25. Astarita, G., *Letter to the editor: "The engineering reality of the yield stress"*, J. Rheol., 34 (1990) 275-277.
26. Papanastasiou, T.C., *Flow of materials with yield*, J. Rheol., 31 (1987) 385-404.
27. Ellwood, K.R.J., Georgiou, G.C., Papanastasiou, T.C., Wilkes, J O, *Laminar jets of Bingham-plastic liquids*, J. Rheol., 34 (1990) 787-812.
28. Abdali, S.S., Mitsoulis, E., Markatos, N.C., *Entry and exit flows of Bingham fluids*, J. Rheol., 36 (1992) 389-407.
29. Mitsoulis, E., Abdali, S.S., Markatos, N.C., *Flow simulation of Herschel-Bulkley fluids through extrusion dies*, Can. J. Chem. Eng., 71 (1993) 147-160.
30. Loest, H., Lipp, R., Mitsoulis, E., *Numerical flow simulation of viscoplastic slurries and design criteria for a tape casting unit*, J. Amer. Ceram. Soc., 77 (1994) 254-262.
31. Blackery, J., Mitsoulis, E., *Creeping flow of a sphere in tubes filled with a Bingham plastic material*, J. Non-Newtonian Fluid Mech., 70 (1997) 59-77.
32. Beaulne, M., Mitsoulis, E., *Creeping flow of a sphere in tubes filled with Herschel-Bulkley fluids*, J. Non-Newtonian Fluid Mech., 72 (1997) 55-71.
33. Pham, T.V., Mitsoulis, E., *Entry and exit flows of Casson fluids*, Can. J. Chem. Eng., 72 (1994) 1080-1084.
34. Pham, T.V., Mitsoulis, E., *Viscoplastic flows in ducts*, Can. J. Chem. Eng., 76 (1998) 120-125.
35. Zisis, Th., Mitsoulis, E., *Flow of Bingham plastics in a lid-driven square cavity*, J. Non-Newtonian Fluid Mech., 101 (2001) 173-180.

36. Zisis, Th., Mitsoulis, E., *Viscoplastic flow around a cylinder kept between parallel plates*, J. Non-Newtonian Fluid Mech., 105 (2002) 1-20.
37. Matsoukas, A., Mitsoulis, E., *Geometry effects in squeeze flow of Bingham plastics*, J. Non-Newtonian Fluid Mech., 109 (2003) 231-240.
38. Mitsoulis, E., Matsoukas, A., *Free surface effects in squeeze flow of Bingham plastics*, J. Non-Newtonian Fluid Mech., 129 (2005) 182-187.
39. Mitsoulis, E., *On creeping drag flow of a viscoplastic fluid past a circular cylinder: wall effects*, Chem. Eng. Sci., 59 (2004) 789-800.
40. Mitsoulis, E., Huilgol, R.R., *Entry flows of Bingham plastics in expansions*, J. Non-Newtonian Fluid Mech., 122 (2004) 45-54.
41. Chatzimina, M., Georgiou, G.C., Argyropaidas, I., Mitsoulis, E., Huilgol, R.R., *Cessation of Couette and Poiseuille flows of a Bingham plastic and finite stopping times*, J. Non-Newtonian Fluid Mech., 129 (2005) 117-127.
42. Chatzimina, M., Xenophontos, C., Georgiou, G., Argyropaidas, I., Mitsoulis, E., *Cessation of annular Poiseuille flows of Bingham plastics*, J. Non-Newtonian Fluid Mech., 142 (2007) 135-142.
43. Mitsoulis, E., Marangoudakis, S., Spyrtos, M., Zisis, Th., Malamataris, N.A., *Pressure-driven flows of Bingham plastics over a square cavity*, J. Fluids Eng., 128 (2006) 993-1003.
44. Mitsoulis, E., *Annular extrudate swell of pseudoplastic and viscoplastic fluids*, J. Non-Newtonian Fluid Mech., 141 (2007) 138-147.
45. Burgos, G.R., Alexandrou, A.N., Entov, V., *On the determination of yield surfaces in Herschel-Bulkley fluids*, J. Rheol., 43 (1999) 463-483.
46. Burgos, G.R., Alexandrou, A.N., *Flow development of Herschel-Bulkley fluids in a sudden three-dimensional square expansion*, J. Rheol., 43 (1999) 485-498.
47. Alexandrou, A.N., McGilvray, T.M., Burgos, G., *Steady Herschel-Bulkley fluid flow in three-dimensional expansions*, J. Non-Newtonian Fluid Mech., 100 (2001) 77-96.
48. Tsamopoulos, J.A., Chen, M.F., Borkar, A.V., *On the spin-coating of viscoplastic fluids*, Rheol. Acta, 35 (1996) 597-615.
49. Smyrniotis, D.N., Tsamopoulos, J.A., *Squeeze flow of Bingham plastics*, J. Non-Newtonian Fluid Mech., 100 (2001) 165-190.
50. Dimakopoulos, Y., Tsamopoulos, J., *Transient displacement of a viscoplastic material by air in straight and suddenly constricted tubes*, J. Non-Newtonian Fluid Mech., 112 (2003) 43-75.
51. Karapetsas, G., Tsamopoulos, J.A., *Transient squeeze flow of viscoplastic materials*, J. Non-Newtonian Fluid Mech., 133 (2006) 35-56.
52. Dimakopoulos, Y., Tsamopoulos, J., *Transient displacement of Newtonian and viscoplastic liquids by air in complex tubes*, J. Non-Newtonian Fluid Mech., 142 (2007) 162-182.

53. Wuensch, O., *Experimentelle Bestimmung Binghamsher Stoffparameter*, Rheol. Acta, 29 (1990) 163-169.
54. Wuensch, O., *Oscillating sedimentation of spheres in viscoplastic fluids*, Rheol. Acta, 33 (1994) 292-302.
55. Atapattu, D.D., Chhabra, R.P., Uhlherr, P.H.T., *Wall effect for spheres falling at small Reynolds number in a viscoplastic medium*, J. Non-Newtonian Fluid Mech., 38 (1990) 31-42.
56. Atapattu, D.D., Chhabra, R.P., Uhlherr, P.H.T., *Creeping sphere motion in Herschel-Bulkley fluids: flow field and drag*, J. Non-Newtonian Fluid Mech., 59 (1995) 245-265.
57. Liddell, P.V., Boger, D.V., *Yield stress measurements with the vane*, J. Non-Newtonian Fluid Mech., 63 (1996) 235-261.
58. Pashias, N., Boger, D.V., Summers, J., Glenister, D.J., *A fifty cent rheometer for yield stress measurement*, J. Rheol., 40 (1996) 1179-1189.
59. Hariharaputhiran, M., Shankar Subramanian, R., Campbell, G.A., Chhabra, R.P., *The settling of spheres in a viscoplastic fluid*, J. Non-Newtonian Fluid Mech., 79 (1998) 87-97.
60. Meeten, G.H., *Yield stress of structured fluids measured by squeeze flow*, Rheol. Acta, 39 (2000) 399-408.
61. Jossic, L., Magnin, A., *Drag and stability of objects in a yield stress fluid*, AIChE J., 47 (2001) 2666-2672.
62. Jossic, L., Briguet, A., Magnin, A., *Segregation under flow of objects suspended in a yield stress fluid and NMR imaging visualization*, Chem. Eng. Sci., 57 (2002) 409-418.
63. Deglo de Besses, B., Magnin, A., Jay, P., *Sphere drag in a viscoplastic fluid*, AIChE J., 50 (2004) 2627-2629.
64. Chan, T.W., Baird, D.G., *An evaluation of a squeeze flow rheometer for the rheological characterization of a filled polymer with a yield stress*, Rheol. Acta, 41 (2002) 245-256.
65. Barnes, H., *The yield stress – a review or ‘παντα ρει’ – everything flows?*, J. Non-Newtonian Fluid Mech., 81 (1999) 133-178.
66. Engmann, J., Servais, C., Burbidge, A.S., *Squeeze flow theory and applications to rheometry: a review*, J. Non-Newtonian Fluid Mech., 132 (2005) 1-27.
67. Frigaard, I.A., Nouar, C., *On the usage of viscosity regularization methods for visco-plastic fluid flow computation*, J. Non-Newtonian Fluid Mech., 127 (2005) 1-26.
68. Institute for Scientific Information, ISI, Web of Science, www.ekt.gr, Dec. 2006.
69. Balmforth, N.J., Frigaard, I.A., *Visco-plastic fluids: from theory to applications*, J. Non-Newtonian Fluid Mech., 142 (2007) 1-3.

70. Bird, R.B., Stewart, W.E., Lightfoot, E.N., *Transport phenomena*, Wiley, New York (1960).
71. Bird, R.B., Hassager, O., Armstrong, R C, *Dynamics of polymeric liquids, Vol. I: fluid mechanics*, 2nd Edition, Wiley, New York (1987).
72. Oldroyd, J.G., *A rational formulation of the equations of plastic flow for a Bingham solid*, Proc. Camb. Philos. Soc., 43 (1947) 100-105.
73. Glowinski, R., *Numerical methods for nonlinear variational problems*, Springer-Verlag, New York (1984).
74. Huilgol, R.R., Panizza, M.P., *On the determination of the plug flow region in Bingham fluids through the application of variational inequalities*, J. Non-Newtonian Fluid Mech., 58 (1995) 207-217.
75. Huilgol, R.R., *Variational inequalities in the flows of yield stress fluids including inertia: theory and applications*, Phys. Fluids, 14 (2002) 1269-1283.
76. Huilgol, R.R., You, Z., *Application of the augmented Lagrangian method to steady pipe flows of Bingham, Casson and Herschel-Bulkley fluids*, J. Non-Newtonian Fluid Mech., 128 (2005) 126-143.
77. Roquet, N., Saramito, P., *An adaptive finite element method for Bingham fluid flows around a cylinder*, Comput. Methods Appl. Mech. Engrg., 192 (2003) 3317-3341.
78. Vinay, G., Wachs, A., Agassant, J.-F., *Numerical simulation of non-isothermal viscoplastic waxy crude oil flows*, J. Non-Newtonian Fluid Mech., 128 (2005) 144-162.
79. Vinay, G., Wachs, A., Agassant, J.-F., *Numerical simulation of weakly compressible Bingham flows: application to the restart of waxy crude oils*, J. Non-Newtonian Fluid Mech., 136 (2006) 93-105.
80. Shangraw, R., Grim, W., Mattocks, A.M., *An equation for non-Newtonian flow*, Trans. Soc. Rheol., 5 (1961) 247-260.
81. Gavrus, A., Ragneau, E., Caestecker, P., *A rheological behaviour formulation of solid metallic materials for dynamic forming processes simulation*, Proc. 4<sup>th</sup> Intern. ESAFORM Conf. Mat. Form., Ed. A.M. Habraken, Universite de Liege, Vol. 1, pp. 403-406 (2001).
82. Hirt, C.W., Nichols, B.D., *Volume of fluid (VOF) method for the dynamics of free boundaries*, J. Comp. Phys., 39 (1981) 201-225.
83. Faxen, O.H., *Forces exerted on a rigid cylinder in a viscous fluid between two parallel fixed planes*, Proc. R. Swed. Acad. Eng. Sci., 187 (1946) 1-13.
84. Adachi, K., Yoshioka, N., *On creeping flow of a visco-plastic fluid past a cylinder*, Chem. Eng. Sci., 28 (1973) 215-226.
85. Deglo de Besses, B., Magnin, A., Jay, P., *Viscoplastic flow around a cylinder in an infinite medium*, J. Non-Newtonian Fluid Mech., 115 (2003) 27-49.

86. Dai, G., Bird, R.B., *Radial flow of a Bingham fluid between two fixed circular disks*, J. Non-Newtonian Fluid Mech., 8 (1981) 349-355.
87. Wilson, S.D.R., *Squeezing flow of a Bingham material*, J. Non-Newtonian Fluid Mech., 47 (1993) 211-219.
88. Zwick, K.J., Ayyaswamy, P.S., Cohen, I.M., *Variational analysis of the squeezing flow of a yield stress fluid*, J. Non-Newtonian Fluid Mech., 63 (1996) 179-199.
89. Adams, M.J., Aydin, I., Briscoe, B.J., Sinha, S.K., *A finite element analysis of the squeeze flow of an elasto-viscoplastic paste material*, J. Non-Newtonian Fluid Mech., 71 (1997) 41-57.
90. Huang, X., Garcia, M.H., *A Herschel-Bulkley model for mud flow down a slope*, J. Fluid Mech., 374 (1998) 305-333.
91. Walton, I.C., Bittleston, S.H., *The axial flow of a Bingham plastic in a narrow eccentric annulus*, J. Fluid Mech., 222 (1991) 39-60.
92. Szabo, P., Hassager, O., *Flow of viscoplastic fluids in eccentric annular geometries*, J. Non-Newtonian Fluid Mech., 45 (1992) 149-169.
93. Shah, V.L., *Blood Flow*, Advances in Transport Processes, Vol. I, Eds. Mujumdar, A.S., Mashelkar, R.A., Halsted Press, Wiley Eastern Ltd., New Delhi (1980) 1-57.
94. Loest, H., Mitsoulis, E., Spauszus, S., *Free surface measurements and numerical simulations of ceramic tape casting*, Interceram, 42 (1993) 80-84.
95. Caswell, B., Tanner, R.I., *Wirecoating die design using finite element methods*, Polym. Eng. Sci., 18 (1978) 416-421.
96. Mitsoulis E., *Fluid flow and heat transfer in wire coating: a review*, Adv. Polym. Technol., 6 (1986) 467-487.
97. Haas, K.U., Skewis, F.H., *The wire coating process: die design and polymer flow characteristics*, ANTEC '74, Soc. Plast. Eng., 20 (1974) 8-12.
98. Mitsoulis, E., Wagner, R., Heng, F.L., *Numerical simulation of wire-coating low-density polyethylene: theory and experiments*, Polym. Eng. Sci., 28 (1988) 291-310.
99. Mitsoulis, E., Kotsos, P., *Numerical simulation of wire coating pseudoplastic and viscoplastic fluids*, ESAFORM 2005 Conference, Cluj-Napoca, Romania, Ed. Banabic, D, Springer Verlag, Heidelberg, in press (2007).
100. Lipscomb, G.G., Denn, M.M., *Flow of Bingham fluids in complex geometries*, J. Non-Newtonian Fluid Mech., 14 (1984) 337-346.
101. Middleman, S., *Fundamentals of polymer processing*, Chapter 10, McGraw-Hill, New York (1977).
102. Gaskell, R.E., *The calendaring of plastic materials*, J. Appl. Mech., 17 (1950) 334-337.

103. Chung, T.-S., *Analysis for the calendering of Bingham plastic fluids*, J. Appl. Polym. Sci., 25 (1980) 967-970.
104. Sofou, S., Mitsoulis, E., *Calendering of pseudoplastic and viscoplastic sheets of finite thickness*", J. Plast. Film & Sheeting, 20 (2004) 185-222.
105. Sofou, S., Mitsoulis, E., *Calendering of pseudoplastic and viscoplastic sheets using the lubrication approximation*, J. Polym. Eng., 24 (2004) 505-522.
106. Mitsoulis, E., Sofou, S., *Calendering pseudoplastic and viscoplastic fluids with slip at the roll surface*, J. Appl. Mech., 73 (2006) 291-299.
107. Sofou, S., *Calendering of viscoplastic materials*, PhD thesis, School of Mining Engineering, Metallurgy, National Technical University of Athens, Athens, Greece (2007).
108. Atkinson, A.V., *Modelling the semisolid processing of metallic alloys*, Prog. Mater. Sci., 50 (2005) 341-412.
109. Barnes, H.A., *Thixotropy – a review*, J. Non-Newtonian Fluid Mech., 70 (1997) 1-33.
110. Doremus, P., Piau, J.-M., *Yield stress fluid. Structural model and transient shear flow behaviour*, J. Non-Newtonian Fluid Mech., 39 (1991) 335-352.
111. Alexandrou, A.N., Georgiou, G., *On the early breakdown of semisolid suspensions*, J. Non-Newtonian Fluid Mech., 142 (2007) 199-206.